Pseudoprogression of Brain Tumors

Stefanie C. Thust, MD,[1,2,3] Martin J. van den Bent, MD, PhD,[4] and
Marion Smits, MD, PhD[5]*

This review describes the definition, incidence, clinical implications, and magnetic resonance imaging (MRI) findings of pseudoprogression of brain tumors, in particular, but not limited to, high-grade glioma. Pseudoprogression is an important clinical problem after brain tumor treatment, interfering not only with day-to-day patient care but also the execution and interpretation of clinical trials. Radiologically, pseudoprogression is defined as a new or enlarging area(s) of contrast agent enhancement, in the absence of true tumor growth, which subsides or stabilizes without a change in therapy. The clinical definitions of pseudoprogression have been quite variable, which may explain some of the differences in reported incidences, which range from 9–30%. Conventional structural MRI is insufficient for distinguishing pseudoprogression from true progressive disease, and advanced imaging is needed to obtain higher levels of diagnostic certainty. Perfusion MRI is the most widely used imaging technique to diagnose pseudoprogression and has high reported diagnostic accuracy. Diagnostic performance of MR spectroscopy (MRS) appears to be somewhat higher, but MRS is less suitable for the routine and universal application in brain tumor follow-up. The combination of MRS and diffusion-weighted imaging and/or perfusion MRI seems to be particularly powerful, with diagnostic accuracy reaching up to or even greater than 90%. While diagnostic performance can be high with appropriate implementation and interpretation, even a combination of techniques, however, does not provide 100% accuracy. It should also be noted that most studies to date are small, heterogeneous, and retrospective in nature. Future improvements in diagnostic accuracy can be expected with harmonization of acquisition and postprocessing, quantitative MRI and computer-aided diagnostic technology, and meticulous evaluation with clinical and pathological data.
Level of Evidence: 3
Technical Efficacy: Stage 2

Despite maximum treatment, glioblastoma remains almost universally fatal with a median survival of 12–14 months.[1] Current best care consists of maximum safe resection, followed by radiotherapy and chemotherapy. A limited benefit has been gained through adoption of temozolomide into standard treatment.[2] In a proportion of patients, the combination of chemotherapy and radiation provokes increased contrast agent uptake and enlargement of residual tumor, or the appearance of new lesions mimicking tumor progression. This phenomenon, referred to as pseudoprogression, has become a major challenge in glioblastoma follow-up, as only surgery or serial imaging is conclusive, which risks a treatment delay for patients with true progressive disease (PD) and uncertainties for patients and treating physicians. Iatrogenic imaging abnormalities are not unique to glioblastoma, and may also occur with radiotherapy in metastasis and lower-grade glioma. The diagnosis of pseudoprogression is not easily made by a single imaging technique, although several modalities and strategies have shown moderately high accuracy, usually in single-center trials. This review will focus on magnetic resonance imaging (MRI) methods in clinical practice and research, discuss technical considerations, and appraise the potential value of computational aids for the distinction of recurrent/progressive brain tumor and chemoradiation effects. It is acknowledged that imaging techniques exist beyond MRI in the form of radioactive tracer studies as potential markers of tumor activity and metabolism.
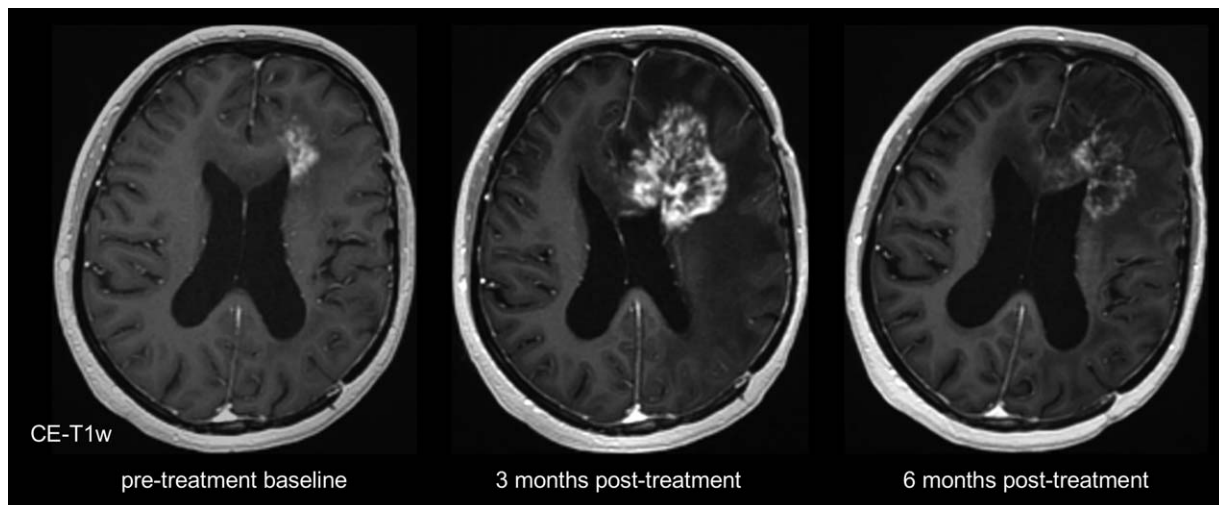
FIGURE 1: Serial contrast-enhanced (CE) T_1-weighted (T_1w) imaging showing increase 3 months and spontaneous decrease 6 months after combined radiotherapy and temozolomide of contrast-enhancement, edema, and mass effect.

Definition, Incidence, and Clinical Aspects of Pseudoprogression

The initial observations that led to the systematic evaluation of pseudoprogression were made by clinicians who noticed some patients clinically deteriorating during or shortly after radiotherapy with increasing lesions on imaging, and with subsequent improvement without intervening treatments.[3] With an initially reported incidence of 10%, such cases were considered relatively infrequent, but still mandated the recommendation not to allow patients who relapsed within 3 months of radiotherapy into phase II studies, as this might result in unreliable study outcomes. This 3-month postradiotherapy exclusion period was clearly arbitrary.

Following the demonstration of improved outcome when temozolomide was added to radiotherapy, several studies reexplored the occurrence of pseudoprogression and treatment-related necrosis. These made the clinical landscape of treatment-induced changes more complex. Chamberlain et al[4] reported more frequent radiation necrosis without evidence of true PD in glioblastoma patients undergoing combined chemoirradiation with temozolomide. This observation was made in a series of 51 glioblastoma patients, 26 of whom showed radiological progression within the first 6 months of the completion of radiotherapy.[4] In 15 of these 26 patients (ie, 29% of all 51 patients), histological evaluation showed only necrosis. Importantly, all reoperated patients were referred for clinical and radiological progression. This incidence, but also the timing of the occurrence of necrosis, is different from historical series, which already suggested an increased rate of radiation necrosis if radiotherapy was combined with chemotherapy.[5,6]

Shortly afterwards, two groups reported on early radiological progression with spontaneous improvement without further treatment. Taal et al[8] described radiological progression at the first scan made 4 weeks after the end of radiotherapy in 36 out of 85 patients. Of these, 18 improved or remained radiologically and clinically stable for 6 months and were diagnosed with pseudoprogression. Clinical signs of deterioration were found in 6 of 18 patients with pseudoprogression, versus 12 of 18 patients with early progressive disease (ePD). Patients with pseudoprogression were significantly younger than those with ePD. Pseudoprogression was found to be unrelated to the size of the radiotherapy field and was observed regardless of initial surgical intervention (biopsy or resection). Brandes et al[9] reported a similar study on 103 patients, and found early radiological signs of progression in 50 of these patients. In 32 (ie, 31% of all 103 patients) the diagnosis of pseudoprogression was made, while in 18 patients (17%) ePD was found. Again, patients with pseudoprogression tended to be less often clinically symptomatic than patients with ePD (34% vs. 57%), and their tumors were more often O^6-methylguanine methyltransferase (MGMT) promotor methylated. These early data have since by and large been confirmed in other series.

What Is Pseudoprogression?

Radiologically, pseudoprogression is defined as a new or enlarging area(s) of contrast agent enhancement occurring early after the end of radiotherapy (eg, within 3–4 months), in the absence of true tumor growth, which subsides or stabilizes without a change in therapy[7] (Fig. 1).

The clinical definitions of pseudoprogression have been quite variable, which may explain some of the differences in reported incidences. Some series required lesions to decrease (partial response) or remain stable for at least 6 months in order to diagnose pseudoprogression,[3,8] while others only used a 2-month interval after the first radiotherapy scan to establish this diagnosis.[9] In a recent article trying to evaluate the role of pseudoprogression in a phase III

trial on bevacizumab in newly diagnosed glioblastoma and using a systematic approach, clinical signs and symptoms were taken as evidence of true PD, which is not supported by the earlier studies on pseudoprogression.[10] The study also used the second MRI scan made as early as 8 weeks later to decide whether true PD was present, and reported a low incidence of pseudoprogression. However, other studies found ongoing pseudoprogression at that point in time. An important contribution of the latter study to this field was the use of an immediate preradiotherapy scan as the baseline for comparison with the postradiotherapy scan. Older series generally used pre- or immediate postsurgery scans for evaluation, which allows surgical changes and tumor progression prior to the start of radiotherapy to weigh in. Another issue that limits the evaluation of pseudoprogression in the modern era is the rapid change to a new line of treatment in radiologically progressing patients. If in that scenario a tumor stabilizes or decreases in size, the underlying cause of resolution of abnormalities cannot be established with any certainty.

Incidence and Outcome

The recently reported incidence of pseudoprogression varies widely, ranging from 9% to 30%.[10–14] Importantly, it takes patients with clinical deterioration and pseudoprogression on average 7 months to recover.[9] With the blurred distinction between pseudoprogression and frank radiation necrosis, it is clear that there is not a specific point in time when a radiological increase equals tumor recurrence with 100% certainty, but the uncertainty is most troublesome in the first 3 months after the end of radiotherapy. It is not inconceivable that many of the anecdotal long-term survivors in trials on recurrent glioblastoma may reflect such cases.

Several studies suggest that patients with pseudoprogression have better survival than the entire group of patients. This type of analysis typically fails to correct for the survivor bias, in that to be diagnosed with pseudoprogression one has to already have survived for a certain period of time.[9,11,12] Some association with MGMT and isocitrate dehydrogenase (IDH) status has been observed in several series, with more frequent pseudoprogression in patients with MGMT promotor methylated and IDH mutated (which are typically also MGMT promotor methylated) tumors. Not unlikely, this is related to the worse outcome in patients with MGMT promotor unmethylated tumors, suffering from earlier tumor progression than patients with MGMT promotor methylation. However, pseudoprogression also occurs in MGMT promotor unmethylated cases. Another series reported 18 cases of radiation necrosis in a series of 159 patients undergoing second surgery for a glioblastoma, in which survival was not improved in patients who suffered from radiation necrosis compared to patients undergoing surgery for PD.[15]

Pseudoprogression Versus Radiation Necrosis

From these early studies, two different patterns emerge: one group with treatment effects observed immediately at the end of radiotherapy, and one group in which clinical and radiological signs are observed at a later stage and who are diagnosed with treatment-related necrosis at the time of second surgery. The common denominator in all these patients is that MRI suggested tumor progression, but outcome proved otherwise. Systematic reports on surgical specimens of cases operated for (early) pseudoprogression are rare. In some early cases frank tumor is visible, making the diagnosis straightforward, but frequently variable amounts of treatment effects and tumor remnants are present.[16] In these clinical series, survival after surgery for pseudoprogression or radiation necrosis is commonly not improved. The presence of cases with mixed morphology consisting of both treatment effects and tumor emphasize the limitations of biopsy to clarify the nature of these clinically challenging cases of early progression. At the histological and at the mechanistic level, early pseudoprogression and radiation necrosis may represent different pathophysiological processes, where some patients with early pseudoprogression continue to develop true radiation necrosis, while others may improve. Probably, radiation therapy treatment induces damage to epithelial cells and local tissue inflammation, which result in edema and abnormal vessel permeability in which vascular endothelial growth factor (VEGF) signaling is upregulated, which in turn can cause an increase in edema seen on T_2-weighted images and/or new or increased contrast agent enhancement.[17] These processes are likely to be enhanced by effective systemic therapies. True radiation necrosis may reflect more severe cases with more extensive tissue and vascular damage, resulting in frank necrosis with fybrinoid necrosis, hyalinization of vessel walls, and reactive gliosis, representing a permanent tissue injury. Radiation necrosis emerges from around 6 months to several years posttreatment. Studies report the frequency of radiation necrosis between 5–25%.[5,18] Its incidence depends on cumulative dose and fractionation, with an increased frequency after stereotactic radiosurgery (SRS).[19]

Treatment for Pseudoprogression and Radiation Necrosis

Awareness of the extent of the clinical problem but also of the limitations of conventional imaging is a major part of the clinical approach. Obtaining a proper baseline scan acquired immediately prior to radiotherapy will prevent some false assessments of (pseudo)progression. It is clear that the immediate postradiotherapy scan should not be used for routine decisions on treatment, but serves as a baseline scan for further management. In clinically asymptomatic patients with radiological progression, treatment will
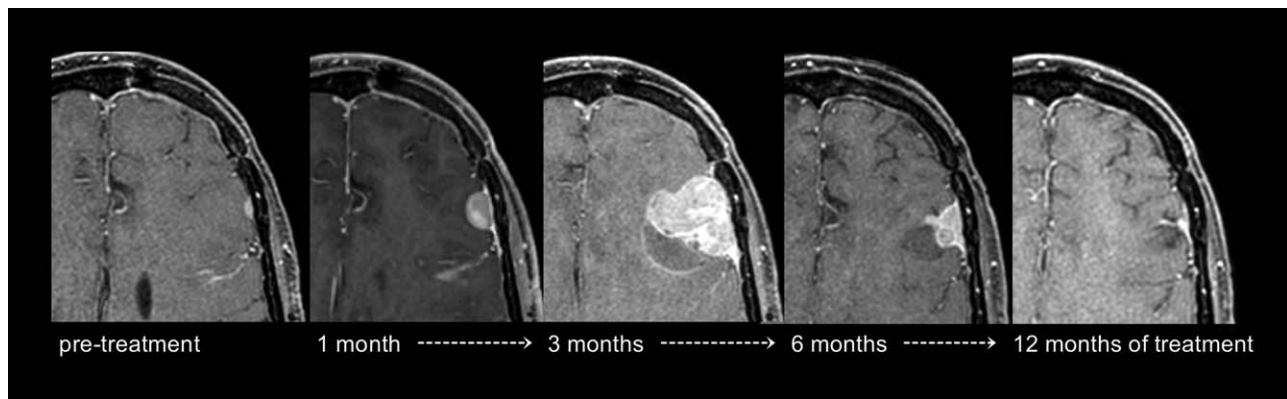
FIGURE 2: Serial postcontrast T_1-weighted imaging of a 34-year-old male patient with dural metastasis from melanoma, treated with pembrolizumab. Treatment was continued despite initial increase of the lesion, which eventually responded. This patient also exhibited extracranial immune response to the treatment. Images courtesy of Drs. M. Jasperse and H. van Thienen at the Netherlands Cancer Institute, Amsterdam (NL).

continue as planned; if clinical deterioration occurs, steroids and surgery will be considered. In challenging cases, surgery can provide greater diagnostic certainty and reduce steroid usage. Steroids are equally effective in controlling signs and symptoms from pseudoprogression and radiation necrosis. In the modern age, although not in all countries, that role has partly been taken over by anti-VEGF agents, in particular bevacizumab.[20] A small series on cediranib, a tyrosine kinase inhibitor of VEGF, suggested a lower frequency of pseudoprogression in cediranib-treated patients.[21] Similarly, the analysis of a large phase III study observed only 2% pseudoprogression in bevacizumab-treated patients, versus 9% in the control arm.[10]

Other Instances of Pseudoprogression and Treatment-Related Effects

Low-Grade Glioma
Treatment-related effects suggesting progression are not limited to glioblastoma. In a recent series, "pseudoprogression" was documented in 13 of 63 (21%) of low-grade glioma patients, occurring within a range of 3–78 months after radiotherapy, with relatively small areas of contrast agent enhancement compared to true PD.[22]

Metastatic Disease
Radiation necrosis is also a well-known phenomenon in patients with brain metastasis treated with SRS. This may occur after a median interval of 7 to 11 months, but sometimes after more than 5 years. Radiation necrosis may explain up to half of the lesions that progress radiologically after SRS.[23,24]

Immunotherapy
Pseudoprogression effects have been observed with use of immunotherapy in cancer[6,25] and concern exists that such changes may also occur in glioblastoma patients treated with immunotherapy (Fig. 2).[26,27] Immunotherapies have shown promising results in the treatment of cancer dissemination to the brain (eg, melanoma), but there is yet limited data on the incidence of pseudoprogression in immune-treated glioblastoma. In the absence of truly effective immunotherapies for glioblastoma this remains largely a speculative problem. The frequency and timing of pseudoprogressive changes has not been fully explored, but based on preliminary evidence most appear to occur within 6 months, consisting of temporary deterioration of treated deposits with subsequent regression or stabilization.[27] It has been suggested that the occurrence of pseudoprogression is associated with an improved clinical prognosis.

Other Effects
Transient contrast agent enhancing abnormalities may manifest in the first months after Gliadel wafer placement.[28]

An entity to be mentioned among probably delayed radiation effects is the SMART (stroke-like migraine attacks after radiotherapy) syndrome. This manifests as recurrent neurological symptoms, including headaches and seizures, associated with (usually unilateral) T_2 hyperintense brain signal abnormalities and gyriform cortical enhancement[29] (Fig. 3). Its pathophysiological mechanism is incompletely understood, but hyperexcitability and endothelial damage are thought to be involved.

Response Criteria
The issue of pseudoprogression led to a change in response evaluation criteria (the Response evaluation in NeuroOncology [RANO] criteria) and to the recommendation not to enroll patients relapsing within 3 months from the end of radiotherapy in trials on recurrent glioblastoma, unless the recurrence is histologically proven or the progressive abnormalities lie outside the radiation field.[7] This comes at the expense of a potential treatment delay for patients with early glioblastoma recurrence within the radiotherapy boundaries.[11] After that, RANO requires a >25% increase in the
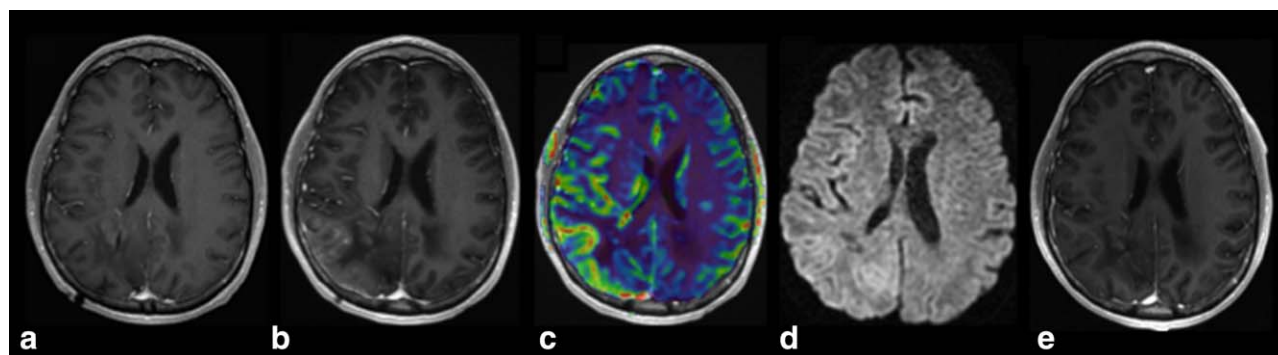
FIGURE 3: Postcontrast T_1-weighted images of a 41-year-old male patient 3 years after radiotherapy for low-grade glioma. Compared with **(A)** there is an increase in—predominantly cortical—enhancement **(B)**. Note that there is also increased rCBV **(C)** and no diffusion abnormalities **(D)**. Follow-up imaging after 2 months **(E)** demonstrates spontaneous resolution of findings, consistent with SMART syndrome.

product of the lesion bidirectional diameter to diagnose PD. One study has questioned whether the RANO classification of small volume (<25%) tumor growth as "stable" disease could negatively impact outcomes.[30] On the contrary, overdiagnosis of PD in patients with only minor glioblastoma growth could result in unwarranted termination of effective treatment. To optimize response assessment for immunotherapy-treated patients, modified so-called iRANO criteria have been devised (Fig. 4), which advocate serial image assessment for enlarging or apparently nonresponding lesions in the first 3–6 months to avoid misdiagnosis of transient phenomena.[27]

Current MRI Approaches to Pseudoprogression

Conventional MRI

Glioblastoma proliferates rapidly, outgrows and newly induces vascularization to maintain oxygenation and nutrient supply. Its newly formed tumor vessels are characterized by endothelial abnormalities and increased permeability,[31,32] which contributes to glioblastoma imaging hallmarks of contrast agent enhancement, central necrosis, and hypervascularity on perfusion studies[33] (Fig. 5). Conventional structural MRI, performed before and after contrast agent injection, does not allow a reliable distinction of
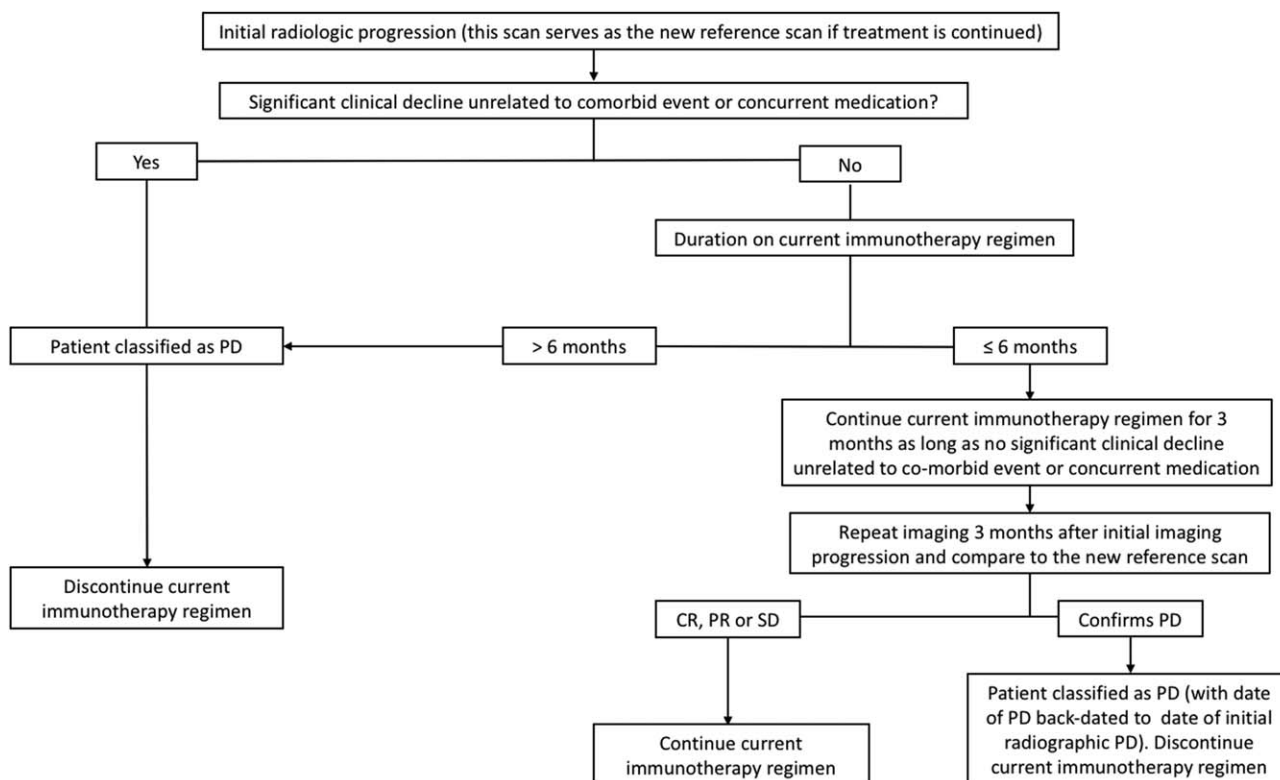

FIGURE 4: iRANO diagnostic algorithm for progressive imaging findings in brain tumor immunotherapy recipients (adapted from Ref. 30).
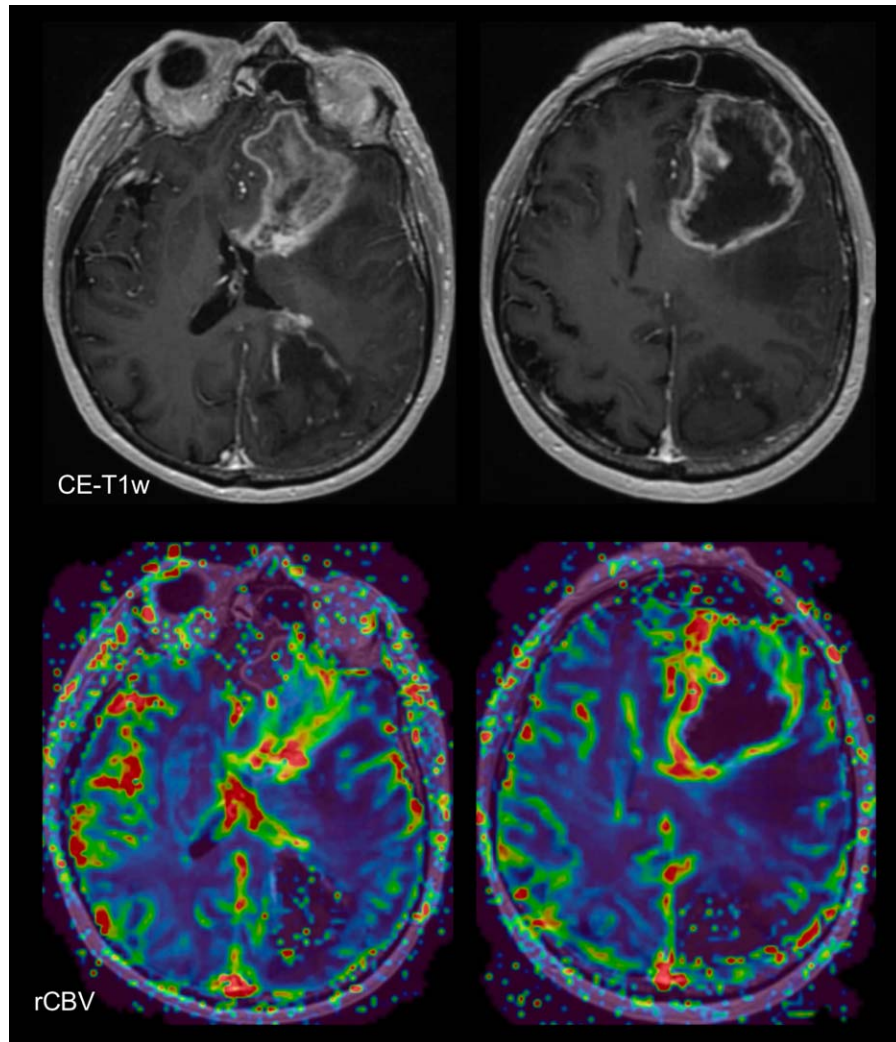
FIGURE 5: MRI features of histopathologically proven glioblastoma: Contrast-enhanced (CE) T_1-weighted (T_1w) sequences shows an enhancing lesion in the left frontal lobe, with areas of central necrosis. There is increased rCBV (green/red) in the enhancing tumor portions. Note there also hemorrhage in the left parieto-occipital region.

pseudoprogression and true PD,[14] as both may share features of mass effect, perilesional edema, and contrast agent enhancement due to blood–brain barrier breakdown. Similarly, for radiation necrosis and tumor, T_1- and T_2-weighted (T_2w) features overlap. Qualitative enhancement descriptors of therapy-induced enhancement patterns ("soap bubble, swiss cheese, moving wave front" (Fig. 6) are subjective and have limited reproducibility.[34] Nevertheless, perceived lesion differences and enhancement morphology[35] could potentially become quantifiable in the era of image texture analysis. It is important to note that contrast-enhanced T_1w image signal is also dependent on contrast dose, injection timing, magnetic field strength, and choice of image sequence.

At present, structural MRI remains the most universally available diagnostic method for monitoring treated glioblastoma,[36] both in clinical practice and as the basis for trials. It fulfils a key role in serial comparison, and should be performed according to standardized protocols to maximize comparability.[37] A recent meta-analysis found the pooled incidence of pseudoprogression on conventional MRI, defined as any transient worsening of lesions on T_1w and/or T_2w images,[38] to be a frequent event: Abbasi et al identified 73 studies in 2603 patients, of which 36% (95% confidence interval [CI], 33–40%) demonstrated some form of pseudoprogression. For those studies (nine studies, $n = 295$) in which the use of RANO criteria was explicitly stated, the pooled incidence was similar 37% (95%, CI 22–52%).[38] Conventional MRI detects T_1w and T_2w/FLAIR lesion changes, but is not sufficient by itself for comprehensive follow-up after brain tumor treatment.

Advanced MRI
Due to the diagnostic limitations of structural MRI, advanced techniques are extensively investigated for their ability to distinguish pseudoprogression and true PD, under the assumption that imaging of pathophysiology will provide more accurate information than merely visualizing—
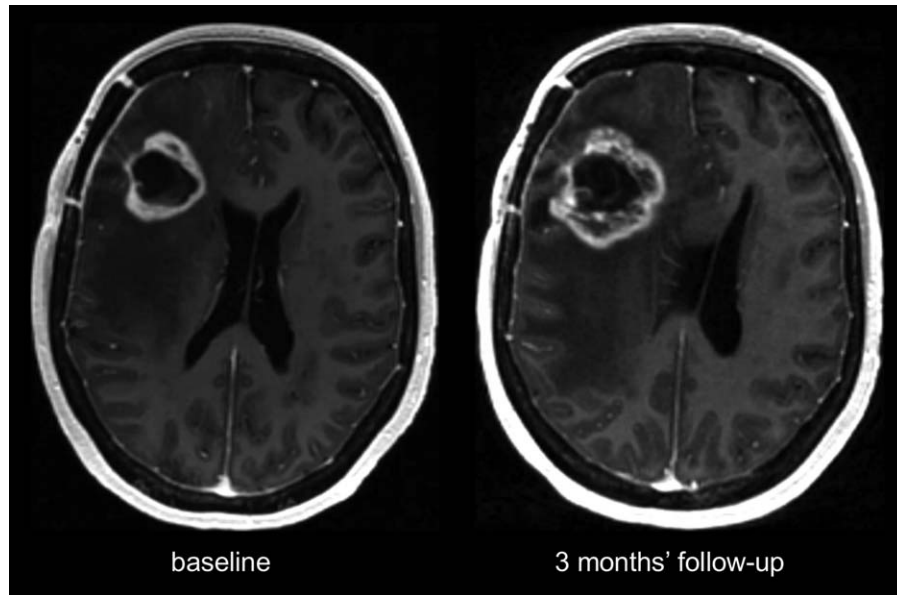
FIGURE 6: Histopathologically confirmed pseudoprogression, where postcontrast T_1-weighted images show a "swiss cheese" or "soap bubble" increase of the margin of the lesion in the right frontal lobe.

unspecific—structural changes. A recent systematic review and meta-analysis identified 45 studies on the diagnostic accuracy of advanced and/or structural MRI in the assessment of adult high-grade glioma response to first-line standard therapy according to the Stupp protocol.[39] The final findings from this meta-analysis were based on 35 studies including a total of 1174 patients with a mean tumor prevalence of 60% (range 31–85%). This meta-analysis showed the highest diagnostic accuracy for MR spectroscopy (nine studies, 203 patients), followed by perfusion imaging (dynamic susceptibility contrast [DSC] perfusion, 18 studies, 708 patients, and dynamic contrast enhanced [DCE] perfusion, five studies, 207 patients). All advanced MRI techniques had higher diagnostic accuracies than anatomical imaging (five studies, 166 patients), for which the pooled sensitivity was 68% (95% CI, 0.51–0.81) and pooled specificity 77% (95% CI, 0.45–0.93) to distinguish between true PD and treatment induced changes.

Perfusion MRI

Perfusion MRI forms a well-established component of glioma follow-up. In a recent survey among 220 European institutions, this technique was regarded as the modality of choice to distinguish radiation effects from tumor progression by the vast majority of institutions.[37]

DSC constitutes the primarily used method for brain tumor perfusion MRI. In two meta-analyses on advanced and perfusion MRI for response assessment, DSC was the most widely used perfusion technique (18/35 and 20/28 studies, respectively).[39,40] DSC perfusion MRI relies on the T_2 and T_2^* shortening effects of gadolinium-based contrast agents and involves rapid imaging to capture the signal changes due to the first passage of an intravenously administered contrast agent bolus (Table 1). The main parameter derived from DSC MRI in the context of brain tumors is the relative cerebral blood volume (rCBV). rCBV is increased in high-grade tumor due to the presence of increased microvascular density and many slow-flowing collateral vessels. Many DSC studies have demonstrated that maximum rCBV is lower in areas of radiation necrosis or pseudoprogression compared to true PD, with reported accuracies in individual studies for the distinction between treatment effects and PD exceeding 90%[33,41–45] (Fig. 7). In two recent meta-analyses performed in the era of the Stupp protocol, pooled sensitivities and specificities for the best-performing parameters were also high: 87% (95% CI, 0.82–0.91) to 90% (95% CI, 0.85–0.94) sensitivity; and 86% (95% CI, 0.77–0.91) to 88% (95% CI, 0.83–0.92) specificity.[39,40] It should be noted that these analyses do not differentiate between late radiation necrosis and the early treatment effects of pseudoprogression. Patel et al assessed the subset of 13 studies reporting on pseudoprogression, although treatment was not always specified in these studies, and found similar diagnostic accuracy, with pooled sensitivity and specificity of 89% (95% CI, 0.83–0.94) and 80% (95% CI, 0.72–0.86) respectively.[40]

An important limitation of the technique is the fact that it is only semiquantitative (hence the term *relative* CBV), and that model assumptions are violated when there is leakage of contrast agent from the intra- to the extravascular compartment, which is invariably the case in enhancing tumor. This problem can be (partly) overcome by the use of a preload bolus to saturate the tissues prior to DSC acquisition and to additionally use leakage correction algorithms[46–49] (Fig. 8). Still, quantification and reproducibility issues hamper the establishment of universal threshold values

TABLE 1. Sample Protocol for Acquiring DCE and DSC Perfusion Imaging

	Dynamic contrast enhanced (DCE) perfusion[136,137]	Dynamic susceptibility contrast (DSC) perfusion[48]
Pulse sequence	T1w	T2*w
Echo time (TE)	2 msec	25–35 msec at 3T; 40–45 msec at 1.5T
Repetition time (TR)	4–7 msec	As fast as possible, preferably ≤ 1500 msec
Flip angle	15 degrees	60–70 degrees
Number of dynamics (duration)	70 (5–15 min)	Baseline (prior to injection) minimum 10; total 120 (1.5–2 min)
Slice thickness	5 mm	3–5 mm
In-plane resolution	1–2 mm^2	2–3 mm^2
Contrast injection rate	2–3 ml/s followed by saline flush	5 ml/s followed by saline flush
Preload contrast bolus	Not necessary; if DSC is also performed, DCE can be acquired during the preload contrast bolus administered for DSC.	Recommended, approximately 5–10 min prior to acquisition

of rCBV for diagnosing pseudoprogression reliably. This is illustrated by the wide range of reported thresholds, from 0.90–2.15 for mean rCBV ratios, and from 1.49–3.10 for maximum rCBV ratios.[40] Of note is that diagnostic accuracy is higher when maximum rCBV is used, which can be explained by intratumoral heterogeneity and the coexistence of tumor and necrotic or inflammatory changes. For the latter reason, methodology has been proposed to quantify spatial heterogeneity, with parameters such as rCBV histogram skewness and kurtosis,[50] or the tumor fractional volume.[42,51] Using single-voxel rCBV ratio thresholding with a cutoff of 1.0 in a study of 25 glioblastoma patients with posttreatment changes, Hu et al were able to determine the histological tumor fraction and to better predict overall survival than when mean rCBV was used.[51] While these methods seem to capture global pathophysiological changes more accurately, the requirement for segmentation of the abnormalities render these time- and labor-consuming, and thus impractical in clinical routine.

An alternative, and less commonly employed technique is DCE MRI, which involves T$_1$-weighted imaging after contrast agent injection over a prolonged period of time (typically 5 minutes or longer) to assess the leakage of contrast agent through the blood–brain barrier (Table 1). The volume transfer constant (K^{trans}) is the most commonly used parameter as a measure of vascular permeability, noting that it is also representative of blood flow and vessel surface area.[52] It should be noted that quantification is highly dependent on the pharmacokinetic models used. K^{trans} tends to be lower in areas of radiation necrosis,[53] as well as in pseudoprogression.[54] Proposed K^{trans} thresholds may vary,[55,56] with none widely established to date (Fig. 9). DCE may also help in cases where DSC is uninterpretable due to susceptibility artifacts, such as hemorrhage or surgical clips, although in such cases DSC with a spin, rather than gradient echo acquisition can also be considered. A commonly employed scenario is the acquisition of DCE during the injection of the preload bolus that is given in preparation for DSC. Diagnostic accuracy of DCE is similar to that of DSC, with pooled sensitivity of 89% (95% CI, 0.78–0.96) to 92% (95% CI, 0.73–0.98) and specificity of 85% (95% CI, 0.76–0.92).[39,40] Due to the variability of
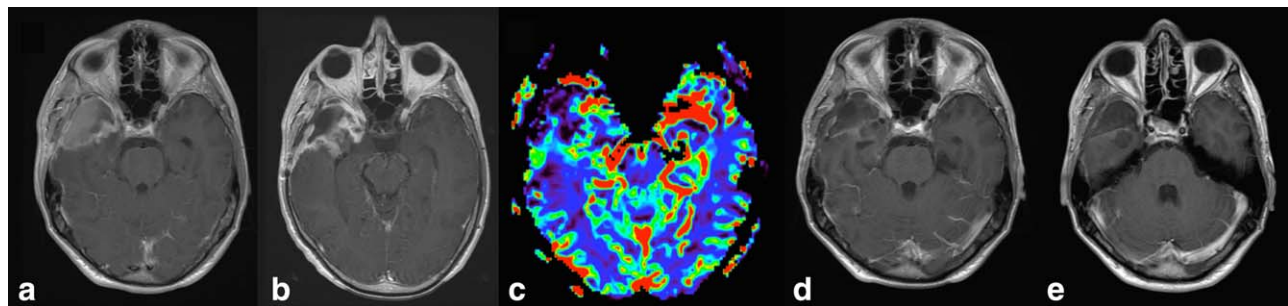
FIGURE 7: Postcontrast T$_1$-weighted images and rCBV map (**C**) demonstrating glioblastoma resection cavity containing blood with early postoperative rim enhancement (**A**), followed by pseudoprogression 2 months later (**B,C**) and spontaneous lesion resolution (**D,E**) over the course of 3 further months.
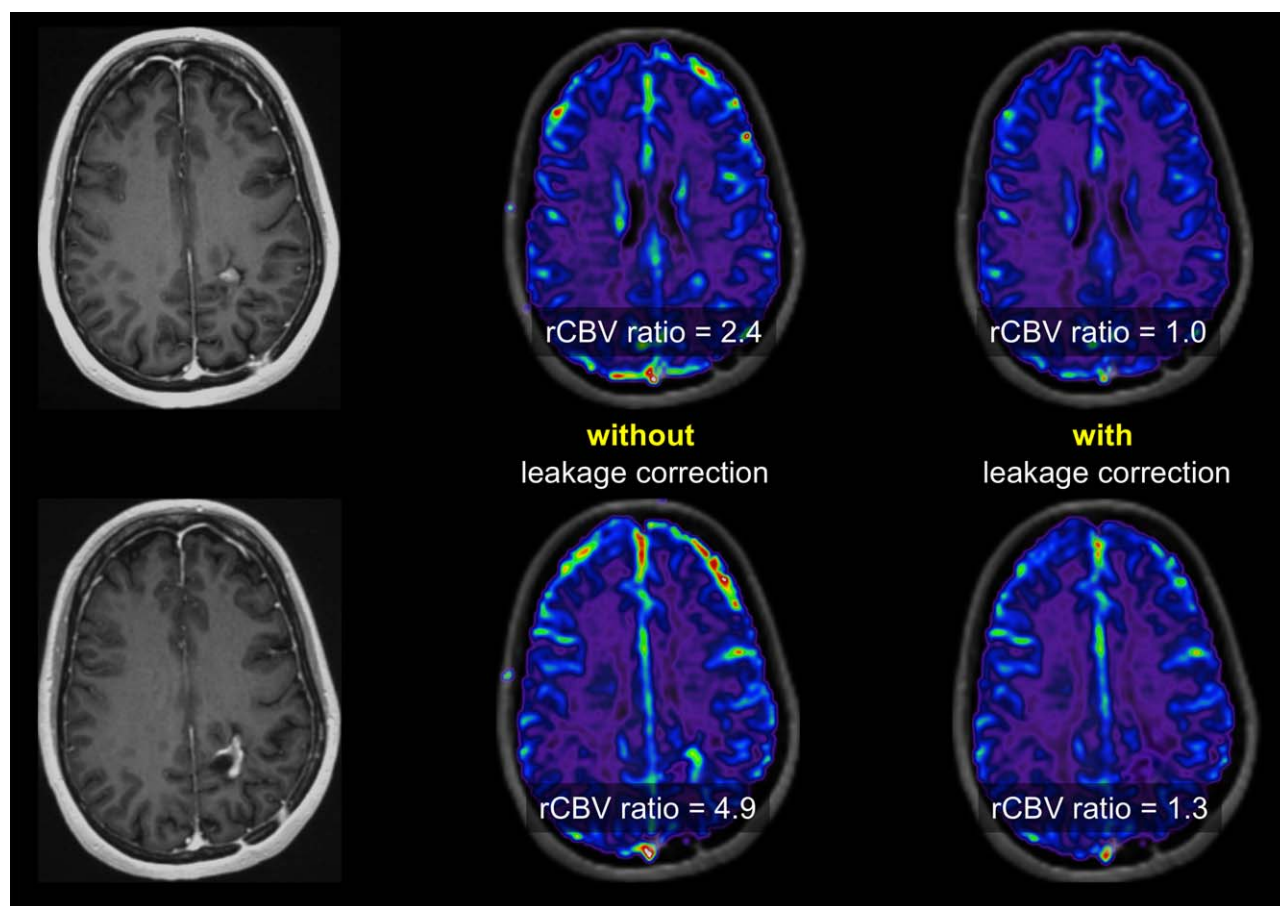
FIGURE 8: Postcontrast T_1-weighted images of the same patient showing an enhancing lesion that remained stable over 1 year follow-up. DSC imaging was acquired with a preload bolus and rCBV maps were calculated. Without leakage correction, rCBV ratios are high; with leakage correction, rCBV ratios are low and more consistent with the clinically observed stable disease than active tumor tissue.

parameters used for quantification, no universal thresholds can be established.

A "static" permeability assessment method, which exploits delayed extravasation of contrast agent, has been introduced in the form of treatment response assessment maps (TRAMS). With this technique, a delayed (>1 hour) postcontrast agent scan is performed to distinguish between regions of contrast agent clearance (hypervascular tumor) and contrast accumulation (nontumor tissues) (Fig. 10). In a study of 150 patients with both primary and metastatic brain tumors, 100% sensitivity and 92% positive predictive value for identifying active tumor was reported.[57] This finding seems to be based on 51 tissue samples, 47 of which included tumor tissue; it is unclear what findings were in the remainder of the 99 patients, and in the absence of an estimate of its specificity, diagnostic accuracy of this technique remains unclear.

A noninvasive perfusion MRI technique is arterial spin labeling (ASL), which uses magnetically labeled blood as an endogenous tracer[58,59] (Fig. 11). Although its use is not widespread for neuro-oncological indications, there are various advantages of this versus the contrast-agent-based perfusion imaging techniques, such as in patients with poor renal function, difficult intravenous access (after chemotherapy), and expected long-term follow-up with the risk of gadolinium retention (pediatric population). Probably the biggest advantage of ASL is that cerebral blood flow (CBF) quantification is not affected by leakage effects with blood–brain barrier disruption, allowing for more accurate quantification.[60] Several studies have shown that DSC and ASL findings correlate well and that accuracy for detecting, classifying, and grading a variety of brain tumors is similar.[61–64] Studies focusing on pseudoprogression/radiation necrosis with ASL specifically are scarce. One study found high correlation between ASL and DSC for differentiating between PD and radiation necrosis.[65] An earlier study reported higher sensitivity of ASL (94%) than DSC perfusion MRI (71%) to identify PD versus radiation necrosis; specificity at this cutoff threshold ratio (1.3), however, was very low with both techniques (50% and 40% with ASL and DSC, respectively).[66]

MRS

The qualitative spectroscopy findings of tumor and therapy effects differ. Recurrent brain neoplasms exhibit elevation of choline (Cho) as a reflection of increased cell membrane
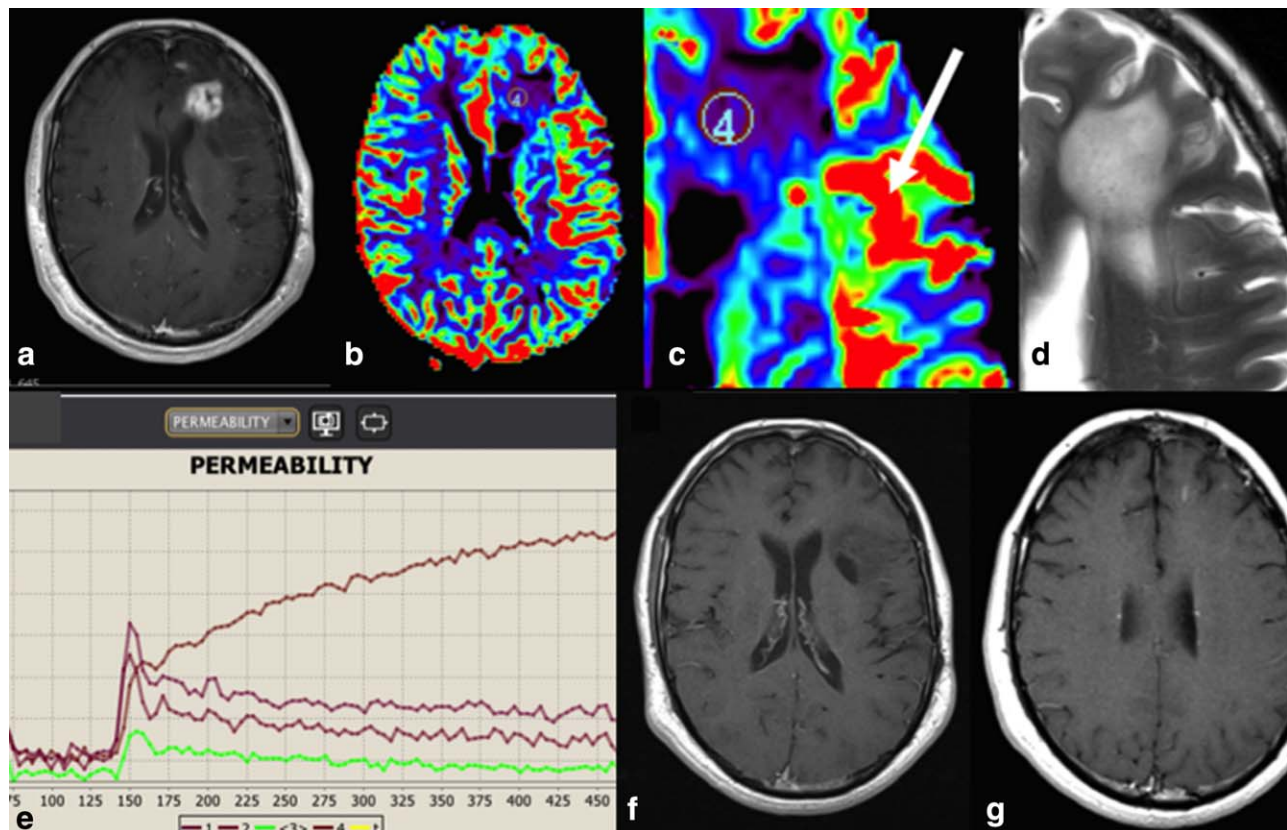
FIGURE 9: Postcontrast images (A), DSC-rCBV maps (B,C), T₂w image (D) and DCE signal intensity curves (E) showing coexisting radiation necrosis (region of interest 4, type 1 curve showing progressive enhancement) and tumor (arrow, type 3 curve showing rapid washout) in a patient with anaplastic astrocytoma 2.5 years following radiotherapy. This was followed by spontaneous enhancing lesion resolution (F,G).

turnover.[67] Features of radiation necrosis include a variable decrease in n-acetyl-aspartate (NAA), lack of pronounced Cho elevation, and the presence of lipid-lactate peaks[68,69] (Fig. 12).

MRS strongly depends on technical parameters: Single voxel spectroscopy measures the average of metabolite concentration within the chosen image volume, which is fraught with inaccuracies and may prevent a clear distinction of PD
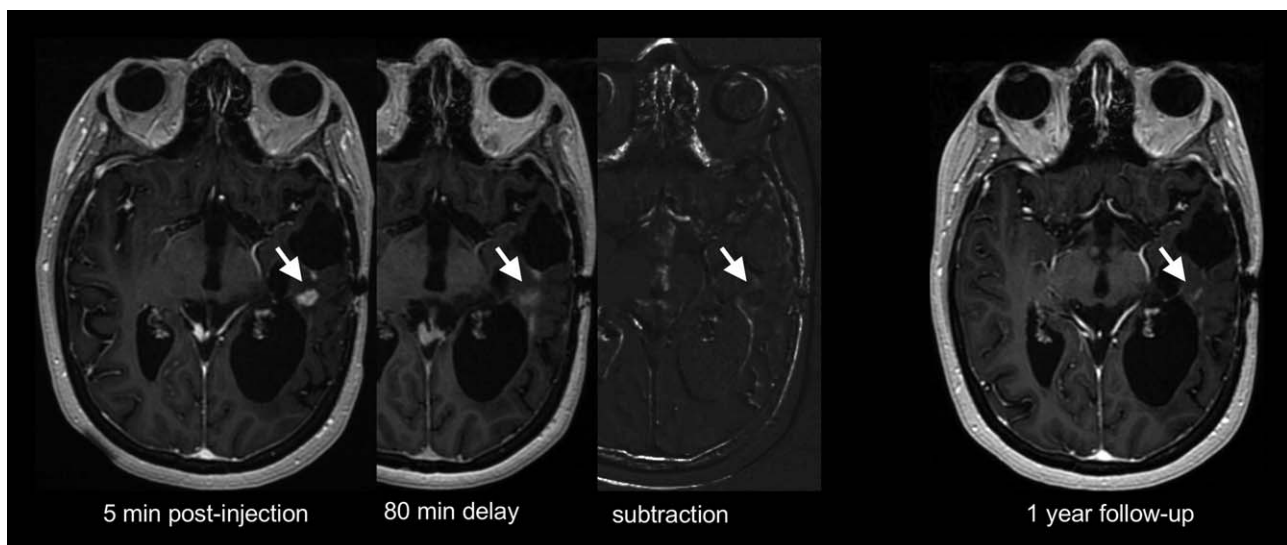

FIGURE 10: Postcontrast T₁-weighted images show an enhancing lesion (arrow) in the left temporal lobe of a patient treated for recurrent glioblastoma. Images obtained 80 minutes postinjection show retention of the contrast agent, resulting in dark signal on the subtraction image, suggestive of nontumoral tissue. One year follow-up shows spontaneous near complete lesion resolution.

FIGURE 11: Postcontrast T$_1$-weighted image (A), DSC derived rCBV (B), and ASL derived CBF (C) maps showing no perfusion abnormality in contrast enhancing radiation necrosis.

from therapy effects. Multivoxel techniques (including chemical shift imaging, CSI) more realistically depict mixed lesions, and can help identify surgical targets. The choice of echo time (TE) can have profound effects on the detection of certain metabolites. For example, lipids are best visible using short (35 msec) echo times, whereas an inverted lactate peak (inconsistently) occurs at a longer echo (144 msec).[70]

Earlier results for the use of MRS in treated brain tumors were positive, whereby several studies achieved a good to excellent (80–97% accuracy) distinction between tumor recurrence and radiation necrosis using Cho/NAA

FIGURE 12: Postcontrast T$_1$-weighted images, DSC perfusion rCBV maps and MRS of radiation necrosis (A–C, MRS with short TE = 30 msec) versus glioblastoma (D–F, MRS with intermediate TE = 144 msec).

and Cho/Cr ratios.[71–73] More recently, Kazda et al and Bulik et al carried out two studies using CSI at one institution, which yielded >90% sensitivity and specificity for the distinction of recurrent glioblastoma from pseudoprogression.[68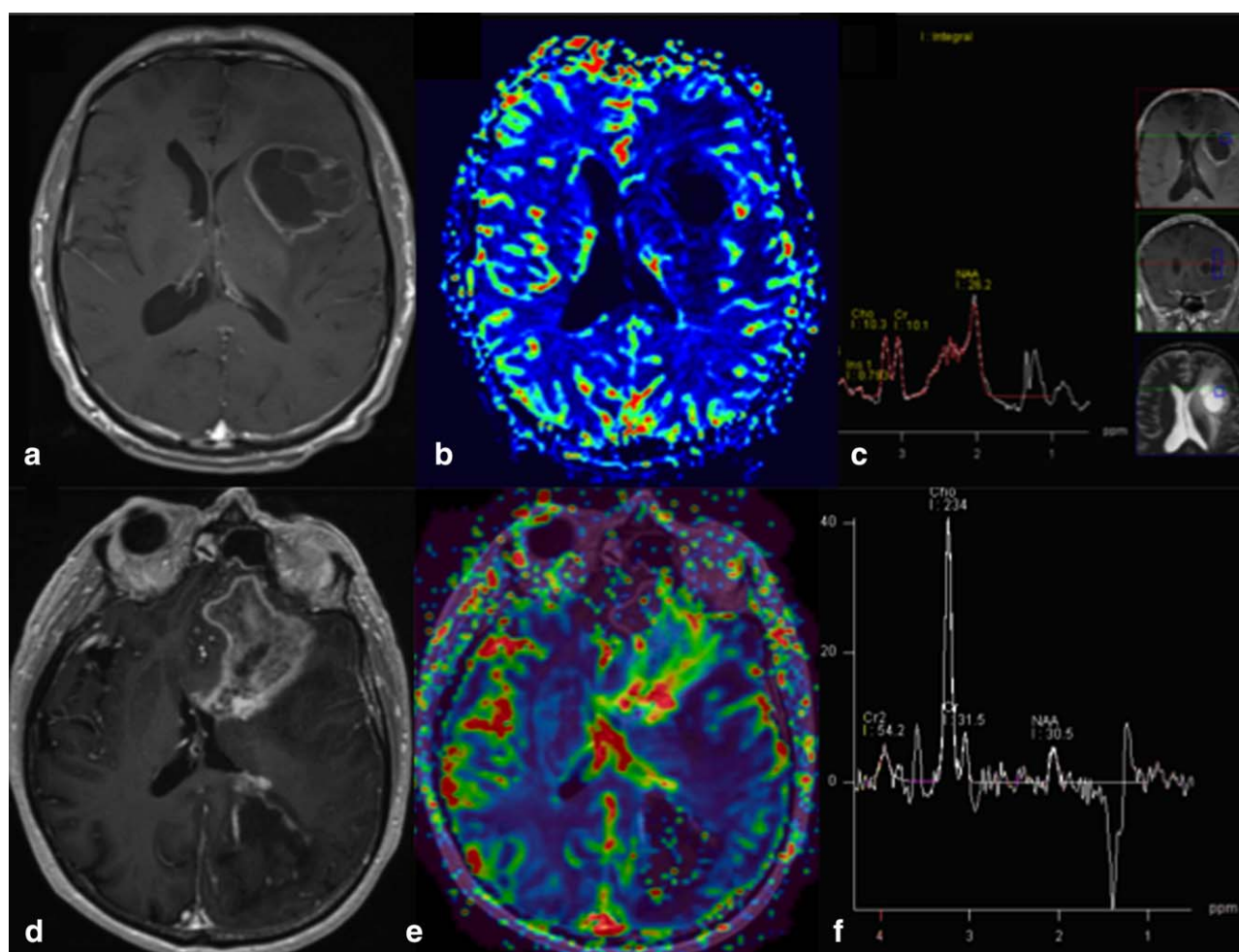,74] This high diagnostic accuracy was confirmed in one meta-analysis, with reported pooled sensitivity of 91% (95% CI, 0.79–0.97) and specificity of 95% (95% CI, 0.65–0.99).[39] In another meta-analysis, Zhang et al reported somewhat lower pooled sensitivity and specificity of the most commonly used Cho/NAA ratios (88% and 86%, respectively) for differentiating recurrent glioma from radiation necrosis, recommending MRS only in a multimodal approach.[75] Nevertheless, MRS has not found very widespread clinical application for this indication. Proposed numerical thresholds vary by as much as 50% of total metabolite concentrations, and may strongly depend on technique and the tumor type examined.[74,76] Some of the studies pursuing threshold cutoffs include mixed tumor types or grades, for which metabolite ratios are known to vary even prior to treatment.[71] The use of ratios rather than absolute metabolite concentrations potentially further limits MRS comparability.

It has been hypothesized that MRS might confer different information to structural MRI by providing details on lesion metabolism and viability. This is supported by the discovery that metabolic tumor volumes only partially overlap with, or may exceed, macroscopic tumor boundaries.[77–79] The question therefore arises as to how far knowledge of metabolic tumor volumes could influence treatment decisions, particularly if discrepant from structural changes.[78]

Diffusion-Weighted Imaging

Water motion is reduced in rapidly growing tissues; diffusion-weighted imaging (DWI) can therefore act as potential biomarker of tumor cellularity.[80] Consistent associations have been shown between glioma apparent diffusion coefficient (ADC) and proliferative indices.[81–83] For treated glioblastomas, true PD has been found to exhibit generally lower ADC values compared with pseudoprogression. Minimum ADC, lower histogram percentiles, but also mean ADC have been proposed as identifiers of pseudoprogression, with trends towards greater sensitivity than specificity.[84–86] ADC thresholds vary between studies and are dependent on b values, with high (3000 s/mm^2) b values potentially being more accurate with a lesser signal-to-noise ratio.[87]

Recent meta-analyses suggested moderate diagnostic performance for diffusion-weighted MRI in differentiating glioma recurrence from radiation necrosis (pooled sensitivity, 71–82%; pooled specificity, 84–87%).[39,88] While somewhat lower than MRS and perfusion MRI techniques, this diagnostic performance is still superior to that of conventional structural imaging.

ADC measurements, particularly using mean values, have limited accuracy when applied to heterogeneous tumors or to necrosing tissue, in which diffusivity may evolve from cytotoxic edema to liquefaction[89]; furthermore, interobserver variations in region of interest placement have the potential to alter quantitative results.

The spatial pattern of ADC values is of diagnostic interest,[89,90] both for a single timepoint assessment and follow-up. Serial voxel-wise mapping of diffusion could be superior to identify subtle focal changes, but entirely depends on accurate coregistration and requires additional processing time.[91,92] Parametric mapping is considered unsuitable for patients with significant changes in mass effect and brain shift between scans.

Diffusion tensor imaging (DTI) parameters, such as high fractional anisotropy in recurrent glioblastoma, may differentiate between tumor and therapy changes, but it remains to be established whether these outperform three-directional DWI.[93] The results are contradictory regarding the ability of DTI to predict glioma relapse sites.[94,95] Multi-band imaging is an emerging technique, which permits rapid acquisition of advanced diffusion sequences using multiple b values.[96] This can be exploited to model tissue microstructure in greater detail, eg, in the form of neurite orientation and dispersion imaging (NODDI). Intravoxel incoherent motion (IVIM) aims to simultaneously measure diffusion and perfusion effects in tissue. Such techniques have shown promising results for preoperative brain tumor characterization, and could be of interest for the identification of pseudoprogression.[97]

A multimodal approach, eg, using a combination of diffusion and perfusion might add accuracy,[98] but does not consistently appear superior. It should be noted that for antiangiogenic therapy (eg, bevacizumab) recipients, diffusion assessment may be confounded, because low ADC can be observed as a feature of coagulative necrosis but also in glioblastoma recurrence.[99]

Novel Methods

Superparamagnetic Iron Oxides (SPIO)

SPIO nanoparticles have been identified as a promising intravenous contrast alternative to gadolinium-based contrast agents. Among these, ferumoxytol received FDA approval in 2009 as a drug to treat iron deficiency anemia. It has since been researched (off label) for various brain imaging indications and has the advantage of no renal excretion. Because nanoparticles are larger than gadolinium compounds, they remain intravascular even where the blood–brain barrier is disrupted; therefore, no leakage correction is required if these are used for perfusion imaging.[100] Ferumoxytol-derived rCBV has been shown to correlate with treated

glioblastoma survival.[100] Quantitative rCBV results obtained from ferumoxytol perfusion MRI appear comparable to or slightly higher than those calculated from a standard dose gadoteridol bolus in human brain.[101] SPIO uptake may assist the characterization of inflammatory processes via localization of macrophage subtypes and as such could be exploited to confirm the efficacy of immunotherapies.[102] Since 2015, ferumoxytol carries an FDA warning, which recommends slow (over 15 minutes) infusion in diluted form to avoid anaphylaxis. A recent publication of 671 cases receiving 3 ml/sec bolus injections reported around 10% adverse reactions (up to 15% for allergy sufferers) but without any life-threatening events identified.[103]

Chemical Exchange Saturation Transfer (CEST)

CEST is an MRI contrast mechanism in development to gain functional information about tumor metabolic processes.[104] The most widely trialed technique for brain tumor imaging is endogenous CEST, aimed at identifying amide proton transfer (APT) as a pH-dependent measure of protein turnover. With this method, a selective ("saturation") radiofrequency pulse is applied to exchangeable solute amide protons, from which the saturation becomes transferred onto surrounding water molecules ("water pool") through chemical exchange and/or dipolar interactions.[105] With progressive saturation, the water signal amplitude of the metabolically active tissue diminishes, which can be depicted as an image. The origins of CEST contrast are complex and incompletely understood, with magnetic cross-relaxation effects (nuclear Overhauser enhancement, NOE) apparently contributing to APT signal in brain tumors.[106,107] Endogenous CEST appears to identify viable aggressive tumor, having shown greater signal towards higher grades and most recently in IDH wildtype gliomas,[108,109] and for this reason could be of interest for follow-up of treated brain tumors. In preclinical research, Zhou et al recently distinguished glioma and radiation necrosis and were able to demonstrate a serial glioma APT signal reduction subsequent to treatment.[110] More recently, two human studies achieved a statistically significant separation of glioblastoma from pseudoprogression (Ma et al, $n = 32$), and of metastases from radiation necrosis (Mehrabian et al, $n = 16$) at 3T using amide and NOE contrasts, respectively.[111,112]

Texture Analysis and Machine Learning

"Texture" refers to the spatial arrangement of signal intensities in an image. Texture analysis is a summary term for computational methods that assess and quantify imaging features beyond what can be observed by the human eye. First-order statistics are the simplest method, consisting of an extraction of image signal intensities from a histogram.[113] From this, parameters such as mean and standard deviation as well as curve shape (skewness, kurtosis) can be

calculated. Second-order statistics assess the relationship between two image pixels; third- and higher-order statistics evaluate three or more pixel relationships to identify more complex image patterns. This can be applied as computer-learning methods, which operate by progressively eliminating nonspecific traits ("classifiers") from a learning sample until the most unique traits are selected. The learned knowledge is subsequently tested in an independent sample for validation, a method that has already shown potential for brain tumor differential diagnosis and glioma subtyping.[114,115] First-order features of ADC and rCBV appear useful for identifying therapy changes in glioblastoma.[50,85]

Chaddad and Tanougast successfully used a second-order method (gray-level co-occurrence matrix, GLCM) to correlate glioblastoma morphology such as the extent of necrosis with survival.[114] GLCM was also trialed for T_1-weighted, T_2-weighted, and T_2-fluid-attenuated inversion recovery (FLAIR) MRI, achieving an accuracy of 86% for the differentiation of glioblastoma from pseudoprogression.[116] Booth et al distinguished pseudoprogression from true PD with >85% accuracy using descriptors of image heterogeneity called Minkowski functionals, further highlighting the potential value of anatomical MRI texture analysis.[117] Learning methods can be adapted to permit more or less liberal classifications, depending on whether sensitivity or specificity is most desirable.[118]

With regard to advanced modalities, Hu et al integrated automated segmentations of anatomical sequences, ADC and DSC derived metrics (rCBV, rCBF) into a support vector machine (SVM) learning model with excellent results (AUC, 0.94).[118] SVM may be useful for distinction of metastases and radiation necrosis.[119] In SVM testing, Cho was suggested as the most discriminatory MRS parameter in early treated glioblastoma but with relatively low (<70%) accuracy.[120]

Discussion

Pseudoprogression is an important clinical problem after brain tumor treatment, interfering not only with day-to-day patient care but also the execution and interpretation of clinical trials. Conventional anatomical MRI is insufficient for distinguishing pseudoprogression from true PD; however, it represents the diagnostic basis for serial lesion measurements. It is recommended to incorporate RANO bidirectional axial measurements into reporting[37] and, where possible, to consider transitioning to volumetric tumor assessment.[121] But the questions of incidence and timing of pseudoprogression are incompletely resolved,[11,38] due to heterogeneity in the radiological and clinical definitions and only scarce histopathological data. As such, the RANO standard is imperfect but widely practicable and can mitigate at least some of the uncertainty.

Advanced MRI allows a higher level of diagnostic certainty, but so far no (combination of) imaging technique(s) has 100% accuracy. Despite the high levels of diagnostic accuracy reported in many advanced MRI studies, it should be noted that these studies are generally small, heterogeneous, and retrospective in nature.

Furthermore, there are varying definitions of pseudoprogression, both in imaging and clinical studies, hampering the interpretation and pooling of published studies. For many of the advanced MRI studies, the gold standard to distinguish pseudoprogression from PD consists of a mixture of serial imaging and biopsy,[68,73] which has inherent inaccuracies. Imaging and clinical follow-up are most commonly used, while histological diagnosis is generally considered the gold standard. Even for those studies where biopsy is performed for histological diagnosis, these may suffer from sampling bias and may incompletely capture mixed lesions. Melguizo-Gavilanes et al also demonstrated the complexity of interpreting surgical samples and highlighted that current criteria for histological confirmation may in fact not be such a robust standard to distinguish pseudoprogression from true PD.[16]

Some advanced MRI techniques are well established in clinical practice, whereas others predominate in research. Potential hurdles to clinical translation can arise from lack of hardware or software, time pressure, or not being trained in using the modality.[37] Countless technical parameters can influence acquisition quality and postprocessing[48]; furthermore, thresholds proposed in the advanced imaging literature are mostly unvalidated, which further contributes to uncertainty. To define sufficiently sensitive and specific values is especially problematic for techniques with small percentage differences in signal for the disease entities to be distinguished. Advanced MRI techniques are not currently incorporated into RANO or other response criteria, but efforts are ongoing to standardize techniques and develop quantitative MRI biomarkers (eg, QIBA/RSNA http://qiba-wiki.rsna.org/index.php/Perfusion,_Diffusion_and_Flow-MRI_Biomarker_Ctte).

Perfusion MRI is the most widely used imaging technique to diagnose pseudoprogression and has high reported diagnostic accuracy. Diagnostic performance of MRS appears to be somewhat higher, but due to its lengthy acquisition time, low spatial resolution, technical challenges, and quality issues such as near surgical clips, MRS is less suitable for the routine and universal application in brain tumor follow-up. Overall, MRS appears highly valuable as an adjunct for identifying therapy effects: it may confer different information and be complementary to structural MRI. The combination of MRS and DWI and/or perfusion imaging seems to be particularly powerful, with diagnostic accuracy reaching 90%,[122,123] and even >90% when all three techniques are used.[124] Again, however, it is important to note that these studies are relatively small, heterogeneous, and limited in number. It also needs to be pointed out that there are other imaging modalities for diagnosing pseudoprogression that are not addressed here. This concerns in particular positron emission tomography (PET) with amino acid tracers. Recent studies reported similar diagnostic accuracy to advanced MRI of fluoro-ethyl-tyrosine (FET) PET of at least 85% for differentiating both typical (within 12 weeks) and late (>12 weeks) pseudoprogression after radiochemotherapy completion from true PD.[125]

DSC and DCE perfusion MRI seem to be more or less equivalent in terms of diagnostic performance, with DSC being faster and much more widely used. One potential, but as yet rarely exploited advantage of DCE, is its higher spatial resolution compared with DSC, allowing a more accurate assessment of mixed lesions consisting of both pseudoprogression and true PD. ASL is proposed as a noninvasive alternative to DSC or DCE, which until recently was considered hardly relevant, as postcontrast imaging is integral to brain tumor follow-up. The recent concerns regarding gadolinium retention and toxicity may require a reevaluation of this routine, especially in young patients and long-term survivors. Physiological imaging with noninvasive techniques, such as ASL and CEST, may gain in importance when these techniques further mature (faster scanning, increased signal-to-noise ratio, higher spatial resolution).

One consideration is whether to include advanced techniques routinely in the brain tumor follow-up imaging protocol. This will depend highly on the logistics and set-up of the institution, particularly the ability to re-call the patient for additional imaging if needed. It can be argued that conventional imaging may suffice, if there is stable disease or partial/complete response. However, even in such cases it may be beneficial to use advanced MRI to identify early signs of malignant transformation.[126] The advantages of routine acquisition of advanced MRI for brain tumor follow-up are the availability of its diagnostic information when needed, a consistency of imaging protocols, and sustaining the experience by the radiographers and radiologists. DSC perfusion MRI is well suited to be performed routinely, as it only takes about 2–3 minutes to acquire, and the contrast agent dose can—especially at 3.0T—be kept low, by splitting a single dose into preload and bolus injection.

The greatest drawback of advanced MRI techniques is the lack of standardization. Variations in equipment, acquisition factors, and postprocessing methods are probably impossible to avoid, but these continue to hamper the comparability between institutions, with great risk of distorting even conventional serial imaging interpretation.[127] For image analysis methods requiring spatial registration, eg, parametric mapping and subtraction techniques,[57]

calculations heavily rely on technical accuracy. This problem affects research trials, for which consensus recommendations have recently been published to promote protocol standardization.[128] With respect to clinical practice, the extent of the effects of method variability is partially unknown, but almost certainly represents a significant factor. As an example, enhancing lesion visibility may be influenced by the injection dose and speed, scan delay, choice of echo time, slice thickness, and patient positioning, all of which may negatively impact measurement accuracy and particularly longitudinal, across-center assessment.[129–131]

Variations in acquisition and postprocessing methodology furthermore preclude the universal implementation of cutoff values into clinical practice.[40] Some recommendations on advanced MRI acquisition do exist, such as for DWI,[132] ASL,[133] and DSC,[48] but are as yet lacking for postprocessing and interpretation. Currently available advanced MRI techniques are generally semiquantitative at best and results may be profoundly altered by mathematical models, such that absolute values cannot be used.[48,134] This is commonly dealt with by normalization to reference values, such as from the contralateral normal-appearing white matter, but there is no consensus on size or positioning of the reference region. Worryingly, such postprocessing details are not consistently reported in diagnostic studies of advanced MRI, rendering their proposed threshold values essentially meaningless.

Notwithstanding these numerous limitations, the available evidence, especially from several meta-analyses, strongly supports the use of advanced MRI techniques for brain tumor follow-up in the context of posttreatment changes. Proposed threshold values in the literature, however, should be applied with great care and are maybe only useful as general guides. Ideally, a particular parameter or threshold value is optimized and validated locally, and all postprocessing methodology is applied consistently within the institution. Ongoing efforts to standardize MRI acquisition and postprocessing may eventually allow for the identification of robust thresholds to be implemented universally. Such efforts are also essential for the development and implementation of computer-aided diagnostic techniques, which show promise in distinguishing pseudoprogression from true PD, but require large data throughput and consistent clinical and pathological evaluation. For the moment, however, much of the implementation of computer-aided diagnostic or advanced image analysis techniques is also hampered by the need for tumor segmentation, which generally requires some form of user-input and which can be time-consuming. Automated segmentation as part of the image processing pipeline would resolve this issue. Additionally, it has been suggested that when using automated segmentation, a correction of errors is possibly superior compared to assisting the algorithm in areas of uncertainty, which could be more efficient for clinical practice.[135]

Conclusion

Advanced MRI, particularly perfusion imaging and/or MRS, needs to be applied for the follow-up of treated brain tumor patients to distinguish pseudoprogression from true PD. While diagnostic performance can be high with appropriate implementation and interpretation, even a combination of techniques does not provide 100% accuracy. Improvements can be expected with harmonization of acquisition and postprocessing, quantitative MRI and computer-aided diagnostic technology, and meticulous evaluation with clinical and pathological data.

Funding

References

1. Koshy M, Villano JL, Dolecek TA, et al. Improved survival time trends for glioblastoma using the SEER 17 population-based registries. J Neurooncol 2012;107:207–212.

2. Stupp R, Hegi ME, Mason WP, et al. Effects of radiotherapy with concomitant and adjuvant temozolomide versus radiotherapy alone on survival in glioblastoma in a randomised phase III study: 5-year analysis of the EORTC-NCIC trial. Lancet Oncol 2009;10:459–466.

3. de Wit MCY, de Bruin HG, Eijkenboom W, Sillevis Smitt PAE, van den Bent MJ. Immediate post-radiotherapy changes in malignant glioma can mimic tumor progression. Neurology 2004;63:535–537.

4. Chamberlain MC, Glantz MJ, Chalmers L, Van Horn A, Sloan AE. Early necrosis following concurrent Temodar and radiotherapy in patients with glioblastoma. J Neurooncol 2007;82:81–83.

5. Ruben JD, Dally M, Bailey M, Smith R, McLean CA, Fedele P. Cerebral radiation necrosis: incidence, outcomes, and risk factors with emphasis on radiation parameters and chemotherapy. Int J Radiat Oncol Biol Phys 2006;65:499–508.

6. Kumar AJ, Leeds NE, Fuller GN, et al. Malignant gliomas: MR imaging spectrum of radiation therapy- and chemotherapy-induced necrosis of the brain after treatment. Radiology 2000;217:377–384.

7. Wen PY, Macdonald DR, Reardon DA, et al. Updated response assessment criteria for high-grade gliomas: response assessment in neuro-oncology working group. J Clin Oncol 2010;28:1963–1972.

8. Taal W, Brandsma D, de Bruin HG, et al. The incidence of pseudoprogression in a cohort of malignant glioma patients treated with chemo-radiation with temozolomide. J Clin Oncol 2007;25(18_suppl): 2009–2009.

9. Brandes A, Tosoni A, Franceschi E, et al. Pseudoprogression after concomitant radio-chemotherapy treatment in newly diagnosed glioblastoma patients and potential correlation with MGMT methylation status. Neuro Oncol 2007;9:529–529.

10. Wick W, Chinot OL, Bendszus M, et al. Evaluation of pseudoprogression rates and tumor progression patterns in a phase III trial of bevacizumab plus radiotherapy/temozolomide for newly diagnosed glioblastoma. Neuro Oncol 2016;18:1434–1441.

11. Radbruch A, Fladt J, Kickingereder P, et al. Pseudoprogression in patients with glioblastoma: clinical relevance despite low incidence. Neuro Oncol 2015;17:151–159.

12. Balaña C, Capellades J, Pineda E, et al. Pseudoprogression as an adverse event of glioblastoma therapy. Cancer Med 2017;6:2858–2866.

13. Topkan E, Topuk S, Oymak E, Parlak C, Pehlivan B. Pseudoprogression in patients with glioblastoma multiforme after concurrent radiotherapy and temozolomide. Am J Clin Oncol 2012;35:284–289.

14. Young RJ, Gupta A, Shah AD, et al. Potential utility of conventional MRI signs in diagnosing pseudoprogression in glioblastoma. Neurology 2011;76:1918–1924.

15. Grossman R, Shimony N, Hadelsberg U, et al. Impact of resecting radiation necrosis and pseudoprogression on survival of patients with glioblastoma. World Neurosurg 2016;89:37–41.

16. Melguizo-Gavilanes I, Bruner JM, Guha-Thakurta N, Hess KR, Puduvalli VK. Characterization of pseudoprogression in patients with glioblastoma: is histology the gold standard? J Neurooncol 2015;123:141–150.

17. Brandsma D, Stalpers L, Taal W, Sminia P, van den Bent MJ. Clinical features, mechanisms, and management of pseudoprogression in malignant gliomas. Lancet Oncol 2008;9:453–461.

18. Rahmathulla G, Marko NF, Weil RJ. Cerebral radiation necrosis: a review of the pathobiology, diagnosis and management considerations. J Clin Neurosci 2013;20:485–502.

19. Ellingson BM, Chung C, Pope WB, Boxerman JL, Kaufmann TJ. Pseudoprogression, radionecrosis, inflammation or true tumor progression? Challenges associated with glioblastoma response assessment in an evolving therapeutic landscape. J Neurooncol 2017;134:495–504.

20. Levin VA, Bidaut L, Hou P, et al. Randomized double-blind placebo-controlled trial of bevacizumab therapy for radiation necrosis of the central nervous system. Int J Radiat Oncol Biol Phys 2011;79:1487–1495.

21. Pinho MC, Polaskova P, Kalpathy-Cramer J, et al. Low incidence of pseudoprogression by imaging in newly diagnosed glioblastoma patients treated with cediranib in combination with chemoradiation. Oncologist 2014;19:75–81.

22. van West SE, de Bruin HG, van de Langerijt B, Swaak-Kragten AT, van den Bent MJ, Taal W. Incidence of pseudoprogression in low-grade gliomas treated with radiotherapy. Neuro Oncol 2017;19:719–725.

23. Narloch JL, Farber SH, Sammons S, et al. Biopsy of enlarging lesions after stereotactic radiosurgery for brain metastases frequently reveals radiation necrosis. Neuro Oncol 2017;19:1391–1397.

24. Fujimoto D, von Eyben R, Gibbs IC, et al. Imaging changes over 18 months following stereotactic radiosurgery for brain metastases: both late radiation necrosis and tumor progression can occur. J Neurooncol 2018;136:207–212.

25. Mullins ME, Barest GD, Schaefer PW, Hochberg FH, Gonzalez RG, Lev MH. Radiation necrosis versus glioma recurrence: conventional MR imaging clues to diagnosis. AJNR Am J Neuroradiol 2005;26:1967–1972.

26. Chiou VL, Burotto M. Pseudoprogression and immune-related response in solid tumors. J Clin Oncol 2015;33:3541–3543.

27. Okada H, Weller M, Huang R, et al. Immunotherapy response assessment in neuro oncology (iRANO): A report of the RANO Working Group. Lancet Oncol 2015;16:e534–e542.

28. Colen RR, Zinn PO, Hazany S, et al. Magnetic resonance imaging appearance and changes on intracavitary Gliadel wafer placement: A pilot study. World J Radiol 2011;3:266–272.

29. Black DF, Morris JM, Lindell EP, et al. Stroke-like migraine attacks after radiation therapy (SMART) syndrome is not always completely reversible: a case series. AJNR Am J Neuroradiol 2013;34:2298–2303.

30. Gzell CE, Wheeler HR, McCloud P, Kastelan M, Back M. Small increases in enhancement on MRI may predict survival post radiotherapy in patients with glioblastoma. J Neurooncol 2016;128:67–74.

31. Bulnes S, Bilbao J, Lafuente JV. Microvascular adaptive changes in experimental endogenous brain gliomas. Histol Histopathol 2009;24:693–706.

32. Plate KH, Mennel HD. Vascular morphology and angiogenesis in glial tumors. Exp Toxicol Pathol 1995;47:89–94.

33. Sugahara T, Korogi Y, Kochi M, et al. Correlation of MR imaging-determined cerebral blood volume maps with histologic and angiographic determination of vascularity of gliomas. AJR Am J Roentgenol 1998;171:1479–1486.

34. Yoo R-E, Choi SH, Kim TM, et al. Independent poor prognostic factors for true progression after radiation therapy and concomitant temozolomide in patients with glioblastoma: subependymal enhancement and low ADC value. AJNR Am J Neuroradiol 2015;36:1846–1852.

35. Reddy K, Westerly D, Chen C. MRI patterns of T1 enhancing radiation necrosis versus tumour recurrence in high-grade gliomas. J Med Imaging Radiat Oncol 2013;57:349–355.

36. Ryken TC, Aygun N, Morris J, et al. The role of imaging in the management of progressive glioblastoma?: A systematic review and evidence-based clinical practice guideline. J Neurooncol 2014;118:435–460.

37. Thust SC, Heiland S, Falini A, et al. Glioma imaging in Europe: A survey of 220 centres and recommendations for best clinical practice. Eur Radiol 2018 [Epub ahead of print].

38. Abbasi AW, Westerlaan HE, Holtman GA, Aden KM, van Laar PJ, van der Hoorn A. Incidence of tumour progression and pseudoprogression in high-grade gliomas: a systematic review and meta-analysis. Clin Neuroradiol 2017 [Epub ahead of print].

39. van Dijken BRJ, van Laar PJ, Holtman GA, van der Hoorn A. Diagnostic accuracy of magnetic resonance imaging techniques for treatment response evaluation in patients with high-grade glioma, a systematic review and meta-analysis. Eur Radiol 2017;27:4129–4144.

40. Patel P, Baradaran H, Delgado D, et al. MR perfusion-weighted imaging in the evaluation of high-grade gliomas after treatment: a systematic review and meta-analysis. Neuro Oncol 2017;19:118–127.

41. Hu LS, Baxter LC, Smith KA, et al. Relative cerebral blood volume values to differentiate high-grade glioma recurrence from posttreatment radiation effect: direct correlation between image-guided tissue histopathology and localized dynamic susceptibility-weighted contrast-enhanced perfusion MR imaging measurements. AJNR Am J Neuroradiol 2009;30:552–558.

42. Gasparetto EL, Pawlak MA, Patel SH, et al. Posttreatment recurrence of malignant brain neoplasm: accuracy of relative cerebral blood volume fraction in discriminating low from high malignant histologic volume fraction. Radiology 2009;250:887–896.

43. Sugahara T, Korogi Y, Tomiguchi S, et al. Posttherapeutic intraaxial brain tumor: the value of perfusion-sensitive contrast-enhanced MR imaging for differentiating tumor recurrence from nonneoplastic contrast-enhancing tissue. AJNR Am J Neuroradiol 2000;21:901–909.

44. Hu LS, Baxter LC, Pinnaduwage DS, et al. Optimized preload leakage-correction methods to improve the diagnostic accuracy of dynamic susceptibility-weighted contrast-enhanced perfusion MR imaging in posttreatment gliomas. Am J Neuroradiol 2010;31:40–48.

45. Kong D-S, Kim ST, Kim E-H, et al. Diagnostic dilemma of pseudoprogression in the treatment of newly diagnosed glioblastomas: the role of assessing relative cerebral blood flow volume and oxygen-6-methylguanine-DNA methyltransferase promoter methylation status. AJNR Am J Neuroradiol 2011;32:382–387.

46. Boxerman JL, Schmainda KM, Weisskoff RM. Relative cerebral blood volume maps corrected for contrast agent extravasation significantly correlate with glioma tumor grade, whereas uncorrected maps do not. AJNR Am J Neuroradiol 2006;27:859–867.

47. Shiroishi MS, Boxerman JL, Pope WB. Physiologic MRI for assessment of response to therapy and prognosis in glioblastoma. Neuro Oncol 2016;18:467–478.

48. Welker K, Boxerman J, Kalnin A, et al. ASFNR recommendations for clinical performance of MR dynamic susceptibility contrast perfusion imaging of the brain. AJNR Am J Neuroradiol 2015;36:E41–51.

49. Paulson ES, Schmainda KM. Comparison of dynamic susceptibility-weighted contrast-enhanced MR methods: recommendations for measuring relative cerebral blood volume in brain tumors. Radiology 2008;249:601–613.

50. Baek HJ, Kim HS, Kim N, Choi YJ, Kim YJ. Percent change of perfusion skewness and kurtosis: a potential imaging biomarker for early treatment response in patients with newly diagnosed glioblastomas. Radiology 2012;264:834–843.

51. Hu LS, Eschbacher JM, Heiserman JE, et al. Reevaluating the imaging definition of tumor progression: perfusion MRI quantifies recurrent glioblastoma tumor fraction, pseudoprogression, and radiation necrosis to predict survival. Neuro Oncol 2012;14:919–930.

52. Tofts PS, Brix G, Buckley DL, et al. Estimating kinetic parameters from dynamic contrast-enhanced T(1)-weighted MRI of a diffusable tracer: standardized quantities and symbols. J Magn Reson Imaging JMRI 1999;10:223–232.

53. Lacerda S, Law M. Magnetic resonance perfusion and permeability imaging in brain tumors. Neuroimaging Clin N Am 2009;19:527–557.

54. Thomas AA, Arevalo-Perez J, Kaley T, et al. Dynamic contrast enhanced T1 MRI perfusion differentiates pseudoprogression from recurrent glioblastoma. J Neurooncol 2015;125:183–190.

55. Nael K, Bauer AH, Hormigo A, et al. Multiparametric MRI for differentiation of radiation necrosis from recurrent tumor in patients with treated glioblastoma. AJR Am J Roentgenol 2018;210:18–23.

56. Bisdas S, Naegele T, Ritz R, et al. Distinguishing recurrent high-grade gliomas from radiation injury: a pilot study using dynamic contrast-enhanced MR imaging. Acad Radiol 2011;18:575–583.

57. Zach L, Guez D, Last D, et al. Delayed contrast extravasation MRI for depicting tumor and non-tumoral tissues in primary and metastatic brain tumors. PLoS One 2012;7:e52008.

58. Heo YJ, Kim HS, Park JE, Choi C-G, Kim SJ. Uninterpretable dynamic susceptibility contrast-enhanced perfusion MR images in patients with post-treatment glioblastomas: cross-validation of alternative imaging options. PLoS One 2015;10:e0136380.

59. Thomsen H, Steffensen E, Larsson E-M. Perfusion MRI (dynamic susceptibility contrast imaging) with different measurement approaches for the evaluation of blood flow and blood volume in human gliomas. Acta Radiol Stockh Swed 1987 2012;53:95–101.

60. Grade M, Hernandez Tamames JA, Pizzini FB, Achten E, Golay X, Smits M. A neuroradiologist's guide to arterial spin labeling MRI in clinical practice. Neuroradiology 2015;57:1181–1202.

61. Järnum H, Steffensen EG, Knutsson L, et al. Perfusion MRI of brain tumours: a comparative study of pseudo-continuous arterial spin labelling and dynamic susceptibility contrast imaging. Neuroradiology 2010;52:307–317.

62. Lehmann P, Monet P, de Marco G, et al. A comparative study of perfusion measurement in brain tumours at 3 Tesla MR: Arterial spin labeling versus dynamic susceptibility contrast-enhanced MRI. Eur Neurol 2010;64:21–26.

63. van Westen D, Petersen ET, Wirestam R, et al. Correlation between arterial blood volume obtained by arterial spin labelling and cerebral blood volume in intracranial tumours. Magma 2011;24:211–223.

64. Hirai T, Kitajima M, Nakamura H, et al. Quantitative blood flow measurements in gliomas using arterial spin-labeling at 3T: intermodality agreement and inter- and intraobserver reproducibility study. AJNR Am J Neuroradiol 2011;32:2073–2079.

65. Ye J, Bhagat SK, Li H, et al. Differentiation between recurrent gliomas and radiation necrosis using arterial spin labeling perfusion imaging. Exp Ther Med 2016;11:2432–2436.

66. Ozsunar Y, Mullins ME, Kwong K, et al. Glioma recurrence versus radiation necrosis? A pilot comparison of arterial spin-labeled, dynamic susceptibility contrast enhanced MRI, and FDG-PET imaging. Acad Radiol 2010;17:282–290.

67. Kamada K, Houkin K, Abe H, Sawamura Y, Kashiwaba T. Differentiation of cerebral radiation necrosis from tumor recurrence by proton magnetic resonance spectroscopy. Neurol Med Chir (Tokyo) 1997;37:250–256.

68. Kazda T, Bulik M, Pospisil P, et al. Advanced MRI increases the diagnostic accuracy of recurrent glioblastoma: Single institution thresholds and validation of MR spectroscopy and diffusion weighted MR imaging. NeuroImage Clin 2016;11:316–321.

69. Kimura T, Sako K, Tohyama Y, et al. Diagnosis and treatment of progressive space-occupying radiation necrosis following stereotactic radiosurgery for brain metastasis: value of proton magnetic resonance spectroscopy. Acta Neurochir (Wien) 2003;145:557–564; discussion 564.

70. Colen RR. Imaging of Brain Tumors, An Issue of Magnetic Resonance Imaging Clinics of North America, E-Book. Amsterdam: Elsevier Health Sciences; 2016.

71. Anbarloui MR, Ghodsi SM, Khoshnevisan A, et al. Accuracy of magnetic resonance spectroscopy in distinction between radiation necrosis and recurrence of brain tumors. Iran J Neurol 2015;14:29–34.

72. Rock JP, Hearshen D, Scarpace L, et al. Correlations between magnetic resonance spectroscopy and image-guided histopathology, with special attention to radiation necrosis. Neurosurgery 2002;51:912–919; discussion 919–920.

73. Weybright P, Sundgren PC, Maly P, et al. Differentiation between brain tumor recurrence and radiation injury using MR spectroscopy. AJR Am J Roentgenol 2005;185:1471–1476.

74. Bulik M, Kazda T, Slampa P, Jancalek R. The diagnostic ability of follow-up imaging biomarkers after treatment of glioblastoma in the temozolomide era: implications from proton MR spectroscopy and apparent diffusion coefficient mapping. BioMed Res Int 2015;2015:641023.

75. Zhang H, Ma L, Wang Q, Zheng X, Wu C, Xu B. Role of magnetic resonance spectroscopy for the differentiation of recurrent glioma from radiation necrosis: a systematic review and meta-analysis. Eur J Radiol 2014;83:2181–2189.

76. Chernov MF, Hayashi M, Izawa M, et al. Multivoxel proton MRS for differentiation of radiation-induced necrosis and tumor recurrence after gamma knife radiosurgery for brain metastases. Brain Tumor Pathol 2006;23:19–27.

77. Lopez CJ, Nagornaya N, Parra NA, et al. Association of radiomics and metabolic tumor volumes in radiation treatment of glioblastoma multiforme. Int J Radiat Oncol Biol Phys 2017;97:586–595.

78. Löbel U, Hwang S, Edwards A, et al. Discrepant longitudinal volumetric and metabolic evolution of diffuse intrinsic Pontine gliomas during treatment: implications for current response assessment strategies. Neuroradiology 2016;58:1027–1034.

79. Jafari-Khouzani K, Loebel F, Bogner W, et al. Volumetric relationship between 2-hydroxyglutarate and FLAIR hyperintensity has potential implications for radiotherapy planning of mutant IDH glioma patients. Neuro Oncol 2016;18:1569–1578.

80. Patterson DM, Padhani AR, Collins DJ. Technology insight: water diffusion MRI—a potential new biomarker of response to cancer therapy. Nat Clin Pract Oncol 2008;5:220–233.

81. Karavaeva E, Harris RJ, Leu K, et al. Relationship between [18F]FDOPA PET uptake, apparent diffusion coefficient (ADC), and proliferation rate in recurrent malignant gliomas. Mol Imaging Biol 2015;17:434–442.

82. Fudaba H, Shimomura T, Abe T, et al. Comparison of multiple parameters obtained on 3T pulsed arterial spin-labeling, diffusion tensor imaging, and MRS and the Ki-67 labeling index in evaluating glioma grading. AJNR Am J Neuroradiol 2014;35:2091–2098.

83. Ellingson BM, Malkin MG, Rand SD, et al. Validation of functional diffusion maps (fDMs) as a biomarker for human glioma cellularity. J Magn Reson Imaging JMRI 2010;31:538–548.

84. Lee WJ, Choi SH, Park C-K, et al. Diffusion-weighted MR imaging for the differentiation of true progression from pseudoprogression following concomitant radiotherapy with temozolomide in patients with newly diagnosed high-grade gliomas. Acad Radiol 2012;19:1353–1361.

85. Song YS, Choi SH, Park C-K, et al. True progression versus pseudoprogression in the treatment of glioblastomas: a comparison study of normalized cerebral blood volume and apparent diffusion coefficient by histogram analysis. Korean J Radiol 2013;14:662–672.

86. Prager AJ, Martinez N, Beal K, Omuro A, Zhang Z, Young RJ. Diffusion and perfusion MRI to differentiate treatment-related changes including pseudoprogression from recurrent tumors in high-grade gliomas with histopathologic evidence. AJNR Am J Neuroradiol 2015; 36:877–885.

87. Chu HH, Choi SH, Ryoo I, et al. Differentiation of true progression from pseudoprogression in glioblastoma treated with radiation therapy and concomitant temozolomide: comparison study of standard and high-b-value diffusion-weighted imaging. Radiology 2013;269:831–840.

88. Zhang H, Ma L, Shu C, Wang Y, Dong L. Diagnostic accuracy of diffusion MRI with quantitative ADC measurements in differentiating glioma recurrence from radiation necrosis. J Neurol Sci 2015;351:65–71.

89. Wang S, Chen Y, Lal B, et al. Evaluation of radiation necrosis and malignant glioma in rat models using diffusion tensor MR imaging. J Neurooncol 2012;107:51–60.

90. Cha J, Kim ST, Kim H-J, et al. Analysis of the layering pattern of the apparent diffusion coefficient (ADC) for differentiation of radiation necrosis from tumour progression. Eur Radiol 2013;23:879–886.

91. Hamstra DA, Galbán CJ, Meyer CR, et al. Functional diffusion map as an early imaging biomarker for high-grade glioma: correlation with conventional radiologic response and overall survival. J Clin Oncol 2008;26:3387–3394.

92. Reimer C, Deike K, Graf M, et al. Differentiation of pseudoprogression and real progression in glioblastoma using ADC parametric response maps. PLoS One 2017;12:e0174620.

93. Wang S, Martinez-Lage M, Sakai Y, et al. Differentiating tumor progression from pseudoprogression in patients with glioblastomas using diffusion tensor imaging and dynamic susceptibility contrast MRI. AJNR Am J Neuroradiol 2016;37:28–36.

94. Price SJ, Jena R, Burnet NG, Carpenter TA, Pickard JD, Gillard JH. Predicting patterns of glioma recurrence using diffusion tensor imaging. Eur Radiol 2007;17:1675–1684.

95. Khalifa J, Tensaouti F, Lotterie J-A, et al. Do perfusion and diffusion MRI predict glioblastoma relapse sites following chemoradiation? J Neurooncol 2016;130:181–192.

96. Wen Q, Kelley DAC, Banerjee S, et al. Clinically feasible NODDI characterization of glioma using multiband EPI at 7 T. NeuroImage Clin 2015;9:291–299.

97. Liu Z-C, Yan L-F, Hu Y-C, et al. Combination of IVIM-DWI and 3D-ASL for differentiating true progression from pseudoprogression of Glioblastoma multiforme after concurrent chemoradiotherapy: study protocol of a prospective diagnostic trial. BMC Med Imaging 2017;17:10.

98. Park JE, Kim HS, Goh MJ, Kim SJ, Kim JH. Pseudoprogression in patients with glioblastoma: assessment by using volume-weighted voxel-based multiparametric clustering of MR imaging data in an independent test set. Radiology 2015;275:792–802.

99. Nguyen HS, Milbach N, Hurrell SL, et al. Progressing bevacizumab-induced diffusion restriction is associated with coagulative necrosis surrounded by viable tumor and decreased overall survival in patients with recurrent glioblastoma. AJNR Am J Neuroradiol 2016;37:2201–2208.

100. Gahramanov S, Muldoon LL, Varallyay CG, et al. Pseudoprogression of glioblastoma after chemo- and radiation therapy: diagnosis by using dynamic susceptibility-weighted contrast-enhanced perfusion MR imaging with ferumoxytol versus gadoteridol and correlation with survival. Radiology 2013;266:842–852.

101. Varallyay CG, Nesbit E, Horvath A, et al. Cerebral blood volume mapping with ferumoxytol in dynamic susceptibility contrast perfusion MRI: Comparison to standard of care. J Magn Reson Imaging JMRI 2018 [Epub ahead of print].

102. McConnell HL, Schwartz DL, Richardson BE, Woltjer RL, Muldoon LL, Neuwelt EA. Ferumoxytol nanoparticle uptake in brain during acute neuroinflammation is cell-specific. Nanomed Nanotechnol Biol Med 2016;12:1535–1542.

103. Varallyay CG, Toth GB, Fu R, et al. What does the boxed warning tell us? Safe practice of using ferumoxytol as an MRI contrast agent. AJNR Am J Neuroradiol 2017;38:1297–1302.

104. Guivel-Scharen V, Sinnwell T, Wolff SD, Balaban RS. Detection of proton chemical exchange between metabolites and water in biological tissues. J Magn Reson 1998;133:36–45.

105. van Zijl PCM, Zhou J, Mori N, Payen J-F, Wilson D, Mori S. Mechanism of magnetization transfer during on-resonance water saturation. A new approach to detect mobile proteins, peptides, and lipids. Magn Reson Med 2003;49:440–449.

106. Shen Y, Xiao G, Shen Z, et al. Imaging of nuclear Overhauser enhancement at 7 and 3 T. NMR Biomed 2017;30.

107. Zaiss M, Windschuh J, Paech D, et al. Relaxation-compensated CEST-MRI of the human brain at 7T: Unbiased insight into NOE and amide signal changes in human glioblastoma. NeuroImage 2015; 112:180–188.

108. Togao O, Yoshiura T, Keupp J, et al. Amide proton transfer imaging of adult diffuse gliomas: correlation with histopathological grades. Neuro Oncol 2014;16:441–448.

109. Jiang S, Zou T, Eberhart CG, et al. Predicting IDH mutation status in grade II gliomas using amide proton transfer-weighted (APTw) MRI. Magn Reson Med 2017;78:1100–1109.

110. Zhou J, Tryggestad E, Wen Z, et al. Differentiation between glioma and radiation necrosis using molecular magnetic resonance imaging of endogenous proteins and peptides. Nat Med 2011;17:130–134.

111. Ma B, Blakeley JO, Hong X, et al. Applying amide proton transfer-weighted MRI to distinguish pseudoprogression from true progression in malignant gliomas. J Magn Reson Imaging JMRI 2016;44:456–462.

112. Mehrabian H, Desmond KL, Soliman H, Sahgal A, Stanisz GJ. Differentiation between radiation necrosis and tumor progression using chemical exchange saturation transfer. Clin Cancer Res 2017;23: 3667–3675.

113. Nailon WH. Texture Analysis Methods for Medical Image Characterisation, Biomedical Imaging. Mao Y, (ed.), 2010. InTech, Available from: http://www.intechopen.com/books/biomedical-imaging/texture-analysis-methods-for-medical-image- characterisation

114. Chaddad A, Tanougast C. Extracted magnetic resonance texture features discriminate between phenotypes and are associated with overall survival in glioblastoma multiforme patients. Med Biol Eng Comput 2016;54:1707–1718.

115. Zacharaki EI, Wang S, Chawla S, et al. Classification of brain tumor type and grade using MRI texture and shape in a machine learning scheme. Magn Reson Med 2009;62:1609–1618.

116. Chen X, Wei X, Zhang Z, Yang R, Zhu Y, Jiang X. Differentiation of true-progression from pseudoprogression in glioblastoma treated with radiation therapy and concomitant temozolomide by GLCM texture analysis of conventional MRI. Clin Imaging 2015;39:775–780.

117. Booth TC, Larkin TJ, Yuan Y, et al. Analysis of heterogeneity in T2-weighted MR images can differentiate pseudoprogression from progression in glioblastoma. PLoS One 2017;12:e0176528.

118. Hu X, Wong KK, Young GS, Guo L, Wong ST. Support vector machine multiparametric MRI identification of pseudoprogression from tumor recurrence in patients with resected glioblastoma. J Magn Reson Imaging JMRI 2011;33:296–305.

119. Larroza A, Moratal D, Paredes-Sánchez A, et al. Support vector machine classification of brain metastasis and radiation necrosis based on texture analysis in MRI. J Magn Reson Imaging JMRI 2015; 42:1362–1368.

120. Imani F, Boada FE, Lieberman FS, Davis DK, Mountz JM. Molecular and metabolic pattern classification for detection of brain glioma progression. Eur J Radiol 2014;83:e100–105.

121. Ellingson BM, Wen PY, Cloughesy TF. Modified criteria for radiographic response assessment in glioblastoma clinical trials. Neurother J Am Soc Exp Neurother 2017;14:307–320.

122. Seeger A, Braun C, Skardelly M, et al. Comparison of three different MR perfusion techniques and MR spectroscopy for multiparametric assessment in distinguishing recurrent high-grade gliomas from stable disease. Acad Radiol 2013;20:1557–1565.

123. Server A, Kulle B, Gadmar ØB, Josefsen R, Kumar T, Nakstad PH. Measurements of diagnostic examination performance using quantitative apparent diffusion coefficient and proton MR spectroscopic imaging in the preoperative evaluation of tumor grade in cerebral gliomas. Eur J Radiol 2011;80:462–470.

124. Matsusue E, Fink JR, Rockhill JK, Ogawa T, Maravilla KR. Distinction between glioma progression and post-radiation change by combined physiologic MR imaging. Neuroradiology 2010;52:297–306.

125. Galldiks N, Law I, Pope WB, Arbizu J, Langen K-J. The use of amino acid PET and conventional MRI for monitoring of brain tumor therapy. NeuroImage Clin 2017;13:386–394.

126. Danchaivijitr N, Waldman AD, Tozer DJ, et al. Low-grade gliomas: do changes in rCBV measurements at longitudinal perfusion-weighted MR imaging predict malignant transformation? Radiology 2008;247:170–178.

127. Reardon DA, Ballman KV, Buckner JC, Chang SM, Ellingson BM. Impact of imaging measurements on response assessment in glioblastoma clinical trials. Neuro Oncol 2014;16(Suppl 7):vii24–35.

128. Ellingson BM, Bendszus M, Boxerman J, et al. Consensus recommendations for a standardized Brain Tumor Imaging Protocol in clinical trials. Neuro Oncol 2015;17:1188–1198.

129. Furutani K, Harada M, Mawlan M, Nishitani H. Difference in enhancement between spin echo and 3-dimensional fast spoiled gradient recalled acquisition in steady state magnetic resonance imaging of brain metastasis at 3-T magnetic resonance imaging. J Comput Assist Tomogr 2008;32:313–319.

130. Kwak H-S, Hwang S, Chung G-H, Song J-S, Choi E-J. Detection of small brain metastases at 3T: comparing the diagnostic performances of contrast-enhanced T1-weighted SPACE, MPRAGE, and 2D FLASH imaging. Clin Imaging 2015;39:571–575.

131. Reuter M, Gerstner ER, Rapalino O, Batchelor TT, Rosen B, Fischl B. Impact of MRI head placement on glioma response assessment. J Neurooncol 2014;118:123–129.

132. Padhani AR, Liu G, Koh DM, et al. Diffusion-weighted magnetic resonance imaging as a cancer biomarker: consensus and recommendations. Neoplasia N 2009;11:102–125.

133. Alsop DC, Detre JA, Golay X, et al. Recommended implementation of arterial spin-labeled perfusion MRI for clinical applications: A consensus of the ISMRM perfusion study group and the European consortium for ASL in dementia. Magn Reson Med 2015;73:102–116.

134. Hu LS, Kelm Z, Korfiatis P, et al. Impact of software modeling on the accuracy of perfusion MRI in glioma. AJNR Am J Neuroradiol 2015; 36:2242–2249.

135. Petersen J, Bendszus M, Debus J, Heiland S, Maier-Hein KH. Effective user interaction in online interactive semantic segmentation of glioblastoma magnetic resonance imaging. J Med Imaging 2017;4:034001.

136. Anzalone, N, Castellano, A, Cadioli, et al. Brain gliomas: multicenter standardized assessment of dynamic contrast-enhanced and dynamic susceptibility contrast MR images. Radiology 2018;:170362.

137. Viallon, M, Cuvinciuc, V, Delattre, B, et al. State-of-the-art MRI techniques in neuroradiology: principles, pitfalls, and clinical applications. Neuroradiology 2015;57:441–467.